Development of Prediction Methods for the Lateral Anchorage Requirements in Metal Building Roof Systems

Jeffrey M. Sears

Thesis submitted to the faculty of the Virginia Polytechnic Institute and State University in partial fulfillment of the requirements for the degree of

Master of Science
In
Civil Engineering

Thomas M. Murray, Chair
W. Samuel Easterling
Raymond H. Plaut

April 30, 2007
Blacksburg, VA

Keywords: Cold Formed Steel, Purlins, Anchorage

Development of Prediction Methods for the Lateral Anchorage Requirements in Metal Building Roof Systems

Jeffrey M. Sears

ABSTRACT

Metal building roof systems with C- or Z-section purlins require restraint to resist lateral forces developed within the roof system under gravity loads. The currently available procedures for predicting these forces have been shown to be inaccurate for sloped roofs and difficult to apply to roof configurations with multiple points of anchorage. A new method has been developed that builds on the previous research and accurately addresses roof slope as well as the use of multiple anchorage devices of finite stiffness. The development of this method relied on a stiffness model, similar to that used by previous researchers, which was updated and calibrated to the results of recently completed tests. The calculation procedure explicitly addresses the location and stiffness of anchorage devices as well as the inherent stiffness of the purlin system to accurately distribute the anchorage forces.

ACKNOWLEDGMENTS

First I would like to thank Dr. Thomas Murray for serving as my advisor and bringing his unsurpassed experience on this topic to this project. His guidance throughout this research and my coursework has been invaluable, and I can't imagine a better leader to work with. Also, I thank Dr. Easterling and Dr. Plaut for serving on my committee. I truly appreciate your time and your efforts. Dr. Michael Seek deserves a special thank you for his willingness to share the findings of his research and to actively support what could have been viewed as competing work.

I want to express my sincere thanks to Dustin Cole, Pat Toney and everyone at Star Building Systems for providing the financial support and the technical resources that made this project possible. This project never would have begun without Dennis Watson (now with BC Steel, formerly my boss at Star) and his impressive ability to see an opportunity and spearhead a solution. I thank you for bringing me on board at the beginning of this project. Research Engineers Inc. graciously provided STAADPro software and invaluable technical support, without which this project would never have been such a success. I thank the members of the AISI Taskgroup on Anchorage and Bracing for all of your probing question and criticisms that drew out the flaws in the research and shaped its final form.

I want to thank my fellow structures graduate students and all the friends I made in Blacksburg and Christiansburg. You have made this experience some of the most enjoyable and fulfilling time in my life. Also, thank you to my daughters Samantha and Mackenzie for your patience (as much as a 2 year old and 2 month old can have) and for being a motivation and inspiration to reach for new goals. Most of all I thank my lovely wife Vicki. I hope that I can repay you for sacrifices you have made. Your love and support are what truly made this all possible, and all worthwhile.

TABLE OF CONTENTS

LIST OF FIGURES

Figure

LIST OF TABLES

Table

CHAPTER I

INTRODUCTION

1.1 BACKGROUND

Metal building systems represent approximately forty percent of non-residential low-rise construction in the United States (MBMA, 2006). Much of the economy in metal building systems comes from the use of cold formed steel purlins in the roof systems. A typical roof system will have longitudinal purlins comprised of cold formed channels or Z-shaped sections supported by gabled or single-sloped steel frames. The purlins are then topped with corrugated steel sheathing that spans in the direction of the roof slope. The roof sheathing is typically attached to the purlin by one of two connection methods: through-fastening or standing seams. With a through fastened system the sheathing bears on the top flange of the purlin and is attached with self drilling screws, typically with integrated washers, which penetrate the sheathing and attach to the purlin top flange. In cases where significant differential thermal movement between the sheathing and the underlying structure occurs, damage to the sheathing around the exposed screw will occur and jeopardize the weather tightness of the roof system. To prevent this issue, or for certain aesthetic preferences, a standing seam system can be used. With this sheathing, a steel clip is attached to the purlin top flange with self drilling screws. The side laps for joining panels then nest over the concealed clip and either interlock or are mechanically seamed to make the attachment.

The roof purlins most commonly consist of cold formed Z-shaped sections. The Z-shapes have the advantage of being able to be nested for shipping and for lapping the sections at the primary supports, see Figure 1.1. This lapped region creates continuity of the section under

bending and provides a doubled cross-section at the location of the greatest shears and moments. The Z-sections used in metal buildings typically range from 6 in. to 12 in. in depth, 2.25 in. to 3.25 in. of flange width, and 0.059 in. to 0.105 in. in thickness, though smaller and larger sections are available. In some cases, C-shaped sections are used for the roof purlins. With C-sections the continuity at the support is achieved by placing the two adjacent members web-to-web as shown in Figure 1.2. The sizes of C-sections used are similar to those for Z-sections.

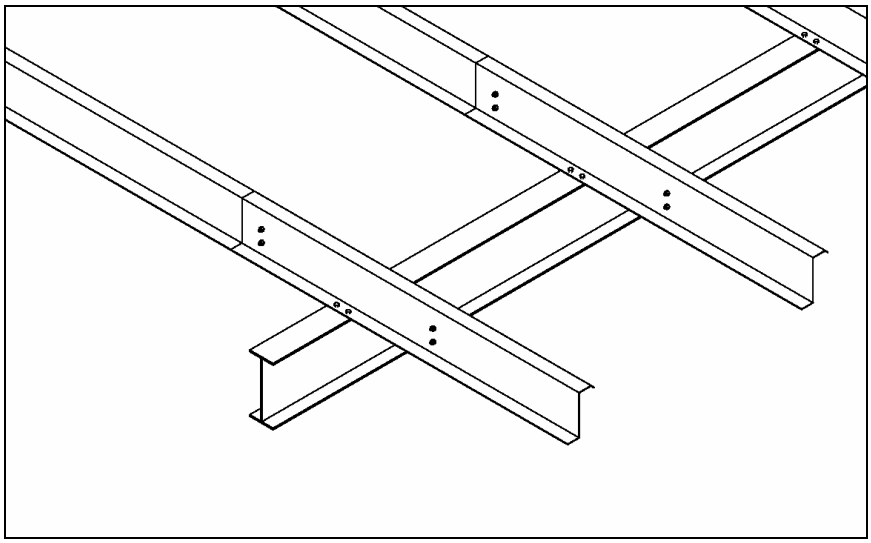

FIGURE 1.1 Continuity Laps with Z-Sections

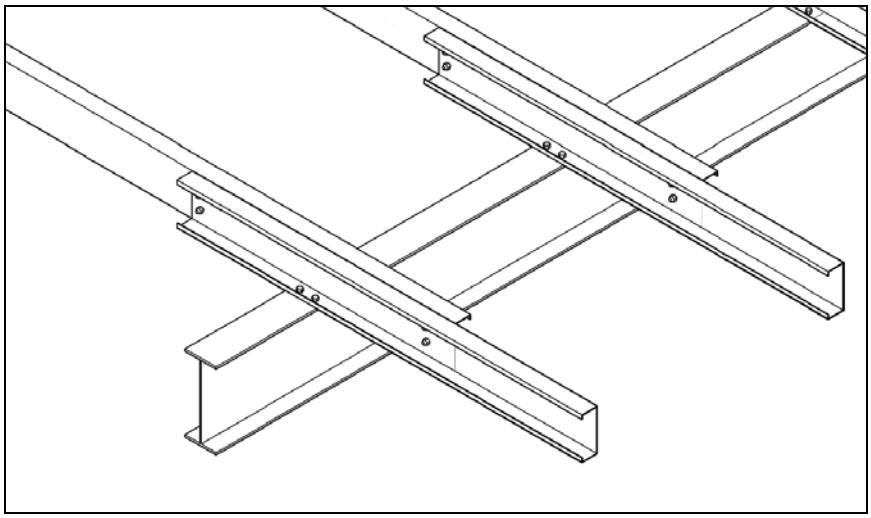

FIGURE 1.2 Continuity Laps with C-Sections

While the use of Z-sections provides significant economy in the system, it also increases the complexity of the flexural analysis. The principal axes of a typical Z-section are inclined relative to the geometric axes by an angle between 10 degrees and 25 degrees, as shown in Figure 1.3. Due to this angle, a load applied parallel to the plane of the web will cause bending about the two principal axes and both vertical and lateral translation of the purlin. In a roof system the sheathing will partially restrain the lateral movement. However, since the sheathing is attached to the top flange, and not at the shear center, torsional moments are introduced.

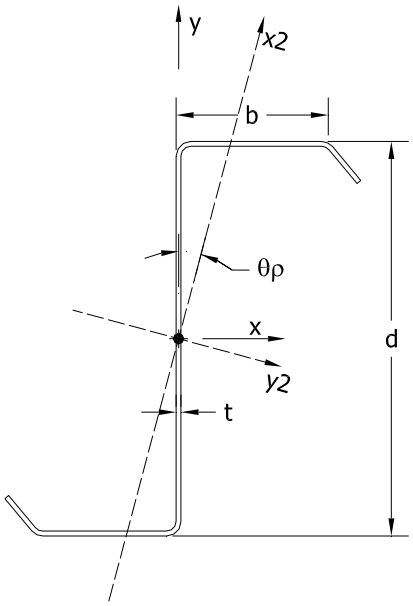

FIGURE 1.3 Z-Section Geometry

For both C- and Z-sections, the roof sheathing bears on the top flange of the purlin. This bearing stress produces a resultant force that is applied some distance away from the plane of the web. The resulting eccentric loading induces torsion in the purlin. For C-sections this effect is amplified because the shear center of the purlin is located beyond the plane of the web as shown in Figure 1.4. The torsion in the member causes the member to twist and translate laterally. The roof sheathing provides partial torsional and lateral restraint to the purlin to resist this torsion.

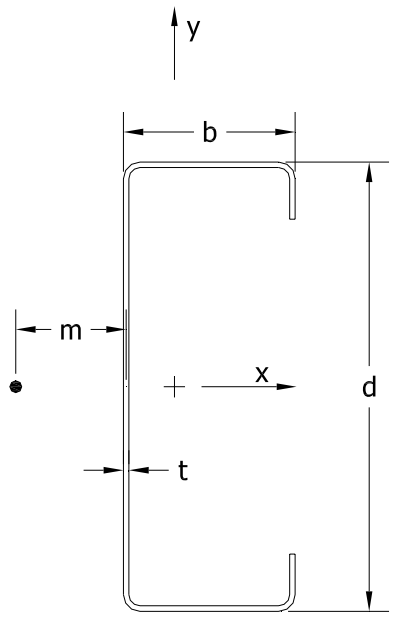

FIGURE 1.4 C-Section Geometry

In typical metal building roofs, the gravity load is primarily applied to the sheathing and acts in a vertical direction. For sloped roofs this load can be divided into two vector components, as shown in Figure 1.5, with one acting perpendicular to the sheathing (and therefore in the plane of the purlin web) and one acting in the plane of the sheathing. The normal component will affect the purlin as discussed above, while the in-plane, or down-slope, component is resisted by the shear stiffness of the sheathing.

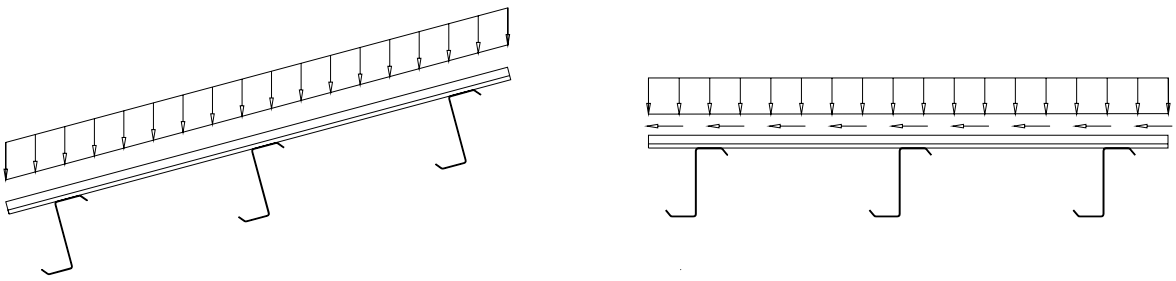

(a) (b)

FIGURE 1.5 Loading of Purlin in Sloped Roofs

Typical design practice in the metal building industry is to design the purlins for the normal component of the applied load and to use the purlin section properties about the geometric axes. This approach assumes that the purlin experiences fully constrained bending and that the lateral and torsional effects are negligible or resisted by some other means. It is common industry practice to assume that the partial lateral and torsional restraint provided by the roof sheathing is adequate to reduce the torsional effect to a negligible level provided the lateral displacements are held within prescribed limits. The torsional moments transferred into the sheathing tend to counteract and are resolved within the roof sheathing, and therefore do not typically require special consideration. However, the lateral forces will accumulate as a shear force in the plane of the diaphragm that must be removed by an external anchorage system.

The most common anchorage systems consist of members attached to purlin webs near the top flange and to the primary structural framing to limit the lateral disp cement of the purlins. These devices may be located at various locations along the purlin span. hen located at the frame lines, the anchorage devices typically consist of either a diagonal ben lip or a multi-

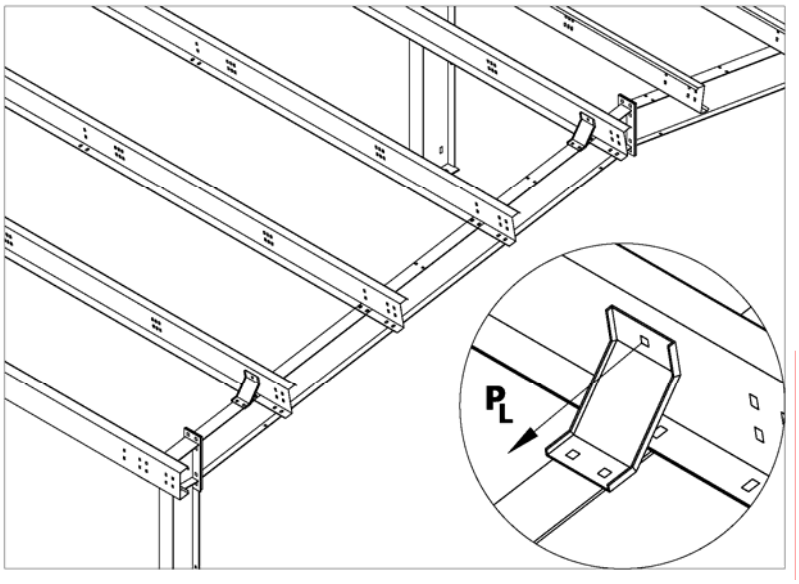

FIGURE 1.6 Purlin Roof with Anchorage Device at Supports

piece welded assembly that is attached to the purlin web and to the top flange of the rafter (see Figure 1.6). For anchorage devices within the purlin span, special detailing considerations need to be addressed and manufacture's preferred details vary greatly.

1.2 LITERATURE REVIEW

Zetlin and Winter (1955) developed a calculation procedure based on bending mechanics to calculate the lateral deflection of an unrestrained Z-purlin due to a load in the plane of the web. In their formulation, the lateral displacement of an unrestrained, uniformly loaded member is found by applying a fictitious force,

$$W_f = \left(I_{xy} \Big/ I_x \right) W \tag{1.1}$$

to a section with a modified moment of inertia of

$$I_{my} = \frac{I_x I_y - I_{xy}^2}{I_x} \tag{1.2}$$

where I_{xy} is the product of inertia, I_x is the moment of inertia with respect to an axis perpendicular to the web, I_y is the moment of inertia with respect to an axis in the plane of the web, and W is the applied load. From this it was concluded that for a Z-purlin that is continuously and rigidly restrained at both flanges, the restraint force must counteract this fictitious lateral force and can be found with the following equation:

$$P_L = \left(I_{xy} \Big/ I_x \right) W \tag{1.3}$$

where P_L is the lateral restraint force. This formulation is for simple spans assuming perfectly rigid lateral restraint at the purlin centroid or at both flanges, concentric loading, and no torsional restraint.

Elhouar and Murray (1985) developed a design procedure that addressed the anchorage forces for Z-purlin roof systems with through fastened sheathing, single or multiple spans, and restraints at the frame lines, 1/3-points, or mid-point of the purlin. Their design equation has the basic form

$$P_L = C\beta W \tag{1.4}$$

where C is a force distribution coefficient and β is an empirical factor based on the results of first order elastic stiffness analyses with frame elements modeling the purlins and truss elements modeling the sheathing. The lateral braces were modeled as truss elements attached at the purlin-to-sheathing connection and anchored to rigid supports. An equation for β was presented for each combination of bracing configuration and simple or multiple spans. For example, for simple spans and restraints at the supports,

$$\beta = \left(\frac{0.220 \cdot b^{1.5}}{n_p^{0.716} d^{0.901} t^{0.6}} \right) \tag{1.5}$$

where n_p is the number of restrained purlin lines, b is the flange width, d is the purlin depth, and t is the purlin thickness. Other equations for β are similar.

The work by Elhouar and Murray (1985) focused on roof systems with zero slope. For implementation in the *North American Specification for the Design of Cold-Formed Steel Members* (AISI, 2001) the equations were modified to account for the roof slope and take the form

$$P_L = C\left(\beta \cos\theta - \sin\theta\right)W \tag{1.6}$$

where θ is the angle between the plane of the roof and the horizontal.

Neubert and Murray (1998) developed a design procedure that attempted to overcome shortcomings in the available formulations related to the roof slope and the diaphragm stiffness.

The proposed design equation had the form

$$P_L = P_o C_1 (\alpha + \gamma) \tag{1.7}$$

where

$$P_o = \left[\left(\frac{I_{xy}}{2I_x} + \frac{b}{3d} \right) \cos\theta - \sin\theta \right] W \tag{1.8}$$

$$\alpha = 1 - C_2 \left(\frac{t}{d} \right) \left(n_p^* - 1 \right) \tag{1.9}$$

$$\gamma = C_3 \log \left(\frac{G'}{2500} \right) \tag{1.10}$$

$$n_p^* = \min \left\{ n_p, 0.5 + \frac{d}{2C_2 t} \right\} \tag{1.11}$$

In this formulation α represents a reduction due to the so-called system effect caused by the torsional deformations of the purlin, and γ is a modifier for shear stiffness of the roof sheathing. The coefficients C1, C2, and C3 were given for each combination of brace configuration and single or multiple spans. These coefficients were determined by regression analysis with data from a computer stiffness model similar to that used by Elhouar and Murray (1985).

Recent work at Virginia Tech by Seek (2007), which was partially concurrent with the new research presented herein, has led to an analytical procedure that utilizes a relative stiffness approach to quantify the behavior of each component of the roof system. Unlike other calculation models, this procedure explicitly considers the rotational stiffness of the purlin to sheathing connection, the flexibility of the purlin web, and the finite stiffness of the anchorage device. The procedure takes a very comprehensive, components based, approach that is computationally intensive and not well suited for use in a design specification.

1.3 SCOPE OF RESEARCH

The goal of this research is to develop an analytical procedure to evaluate the lateral anchorage requirements in metal building systems that overcomes the deficiencies in the currently available methods. The initial phase of this research consisted of developing a computer stiffness model, similar to that used by previous researchers, which could be used for the analyses of anchorage systems where the currently available equations are known to be deficient. This model was calibrated based on the available database of test results. The second phase of the project was to formulate a calculation procedure that accurately predicts the lateral anchorage forces for the majority of situations encountered in the design of metal building roof systems. The formulation of the calculation procedure was based on fundamental mechanics and a simplified stiffness analysis with empirical factors to calibrate the procedure. The computer stiffness model was used to perform parametric studies to investigate the behavior of the purlins and to calibrate the empirical coefficients.

CHAPTER II

COMPUTER MODELING

2.1 OVERVIEW

The goal of this research program was twofold: to develop an efficient and flexible computer stiffness model to analyze purlin anchorage systems, and to develop a simplified analytical procedure that can be implemented in future design specifications. The computer model can be used to analyze special conditions that are beyond the scope of other available procedures. The proposed design provisions include empirical coefficients that allow for the calibration of the procedure. A significant database of test results is available, but it is still insufficient to fully calibrate a new calculation procedure. Because of this, the computer model was developed to extend beyond the tested configurations and provide data for calibrating the calculation procedure.

2.2 SOURCE OF TEST DATA

The computer model was built in a way that closely mimics the physical properties of the actual system, so it was expected that the model behavior should mimic the behavior of the physical system. To verify the model results and to calibrate some of the model properties, the model results were compared to the available test results. Previously proposed calculation procedures were calibrated to tests of flat roof systems performed at the University of Oklahoma by Curtis and Murray (1983) and Sesheppa and Murray (1985). Since the development of the previously proposed procedures, additional tests including sloped roofs have been performed at Virginia Tech by Lee and Murray (2001) and Seek and Murray (2004a).

2.3 SELECTION OF COMPUTER MODEL

The work by Elhouar and Murray (1985) utilized a first order elastic stiffness model with a combination of frame and truss elements to model the roof system. This model was later modified slightly by Neubert and Murray (1998) and was further updated as part of recent research at Virginia Tech (Seek and Murray, 2004b). Seek also developed a separate computer model that utilizes finite elements and agrees very well with the results of tests. Because the computational complexity of this model makes it impractical for modeling large purlin systems or a very large number of models, it was not used for this research. Instead, the space frame/space truss model used by previous researchers was updated to better agree with the new test data.

2.4 DEVELOPMENT OF STIFFNESS MODEL

Preliminary analysis with the model formulated as used by Neubert and Murray (1998) indicated that refinement of the model was needed. The details of the model were adjusted to agree better with the database of test results. The computer stiffness model utilizes linear frame elements to model the purlins and a combination of frame and truss elements to model the sheathing. The material properties of all elements in the model were taken as isotropic steel with a modulus of elasticity of 29,500 ksi and Poisson's ratio of 0.3. Shear deformations and the effects of warping under torsion were neglected. The analysis solution was strictly linear-elastic and neglected all material and geometric non-linearity.

2.4.1 Local and Global Axes

For defining the attributes of the model, a global coordinate system was defined, and a local system of axes was defined for each element type. The global Y-axis was aligned normal to the plane of the roof sheathing, the global Z-axis parallel to the purlin span, and the global X-

axis up the slope of the roof, perpendicular to the purlin web. The local axes of each element were oriented so that the local x-axis lay along the length of the element. The y-axis and z-axis were as shown in Figure 2.1.

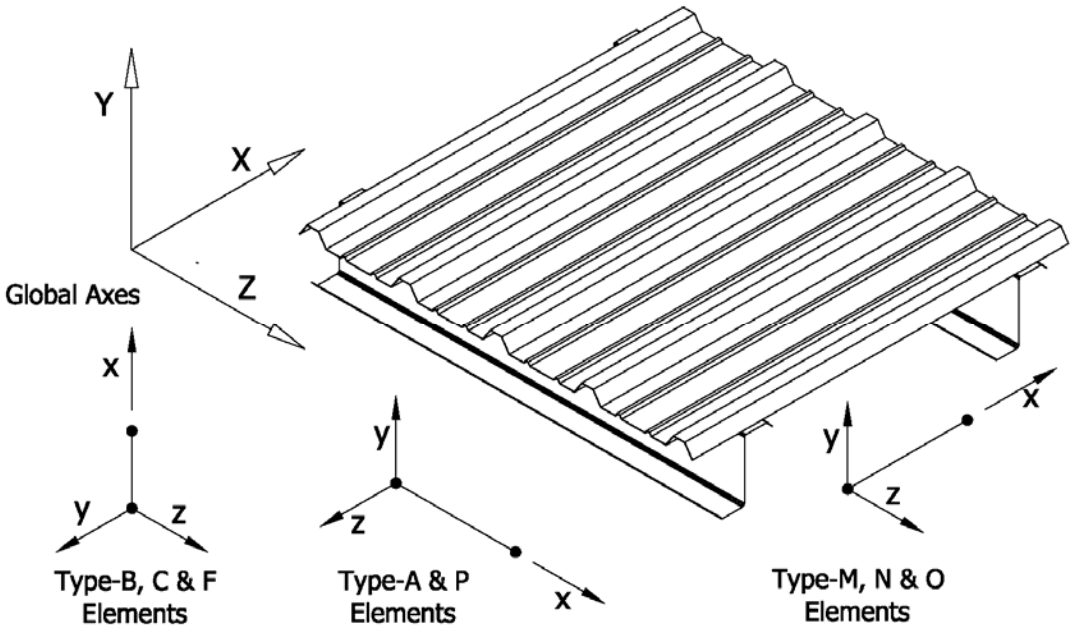

FIGURE 2.1 Local and Global Axes Orientations

2.4.2 Modeling of Purlins

In the computer model, the purlins were represented by a series of frame elements along the axis of the purlin in the plane of the web. The length of the purlin was divided into twelve equal segments to provide nodes for discretizing the roof diaphragm and to provide nodes at one-third points or one-quarter points for the attachment of anchorage devices. The geometry of a purlin was represented by four element types as shown in Figure 2.2.

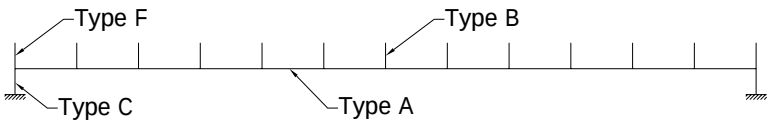

FIGURE 2.2 Purlin Frame Elements

The longitudinal, Type A, elements were assigned the gross area and principal bending moments of inertia of the purlin section being modeled. Table 2.1 shows how the purlin properties given in the *Cold Formed Steel Design Manual* (AISI, 2003) correlate to the properties used in the stiffness model. Also, the axes of the Type A elements were rotated by the principal axis angle, θ_p (see Figure 1.2). The torsional constant, J, was assigned an arbitrarily high value of 10 in.^{4} because the torsional flexibility of the purlin was modeled by the Type B, Type C, and Type F elements. For the scope of the research presented here, a single purlin cross section was used in each roof bay, but the section may vary between bays. Therefore, the element properties input included a definition for each bay. These were named with an index representing each bay (e.g. A1, A2, A3…).

Table 2.1 Type A Element Properties

Stiffness Model Property	***Purlin Property Assigned to Type A Element***
Area	Area
I_{yy}	I_{x2}
I_{zz}	I_{y2}
J	10 in.^{4}
x-axis rotation	θ

For roof systems with multiple spans, the purlins from adjacent bays are typically lapped. To simplify the modeling and the user input, the lapped sections were assumed to extend into each bay for one-twelfth of the bay span. Within this region the area and the moments of inertia of the Type A elements are taken as the sum of the values for the two adjacent bays. The principal axis angle, θ_p, was taken as the average of the two values.

The Type B and Type F elements were included to provide the link between the plane of the roof sheathing and the neutral axis of the purlin and to model the deformations of the purlin web. A moment release for the moments about the y-y axis was added to the element end at the

connection between the Type A elements and the vertical elements. This eliminated the Vierendeel truss action that would artificially stiffen the system. The properties of the Type B elements were assigned to be consistent with a flat plate with a width equal to one-twelfth of the span and a thickness equal to the purlin thickness (see Table 2.2). For simple span purlins and end bays, the Type F elements had properties equal to one-half of the Type B elements. At interior supports in multi-span systems, the purlins are assumed to extend into the adjacent bays. Therefore the properties of the Type F elements were found by the same principles as the Type B elements with the two purlins assumed to act as two non-composite sections. The resulting properties are summarized in Table 2.3.

Table 2.2 Type B Element Properties

Stiffness Model Property	***Purlin Property Assigned to Type B Element***
Area	L/12 x t
I_{yy}	0.0001
I_{zz}	$(L/12 \times t^3)/12$
J	I_{x2}
x-axis rotation	Zero

Table 2.3 Type F Element Properties

Stiffness Model Property	***Purlin Property Assigned to Type F Element @ Ends***	***Purlin Property Assigned to Type F Element @ Laps***
Area	L/24 x t	$(L_1+L_2)/12 \times (t_1 + t_2)$
I_{yy}	0.0001	0.0001
I_{zz}	$(L/24 \times t^3)/12$	$((L_1+L_2)/12 \times (t_1^3+t_2^3))/12$
J	I_{x2}	$(I_{x2})_1 + (I_{x2})_2$
x-axis rotation	Zero	Zero

At the purlin end, the Type C elements provided the connection to the support and modeled the behavior of the lower half of the purlin web in the vicinity of the support. A moment release was assigned to the end of the element at the connection to the Type A and Type F elements to eliminate bending in the plane of the purlin web (M_{zz}-moment). The

properties of the Type C elements were formulated in a similar fashion as the Type F elements. Elhouar and Murray (1985) assigned the bending moment of inertia I_{zz} a value of $Lt^3/2$, which is stiffer than the value related to half the span length, $Lt^3/24$. This was done to minimize the deformation of the Type C elements and force the deformation into the Type F elements, which was believed to better represent the behavior observed during tests. Neubert and Murray (1998) made these elements arbitrarily stiff by setting I_{zz} to a relatively high value of 1 in^4. However, it was found during this research that using properties associated with the end one-twelfth of the span best agreed with tests. The resulting properties for the Type C elements are summarized in Table 2.4.

Table 2.4 Type C Element Properties

Stiffness Model Property	***Purlin Property Assigned to Type C Element @ Ends***	***Purlin Property Assigned to Type C Element @ Laps***
Area	$L/24 \times t$	$(L_1+L_2)/12 \times (t_1 + t_2)$
I_{yy}	0.0001	0.0001
I_{zz}	$(L/24 \times t^3)/12$	$((L_1+L_2)/12 \times (t_1^3+t_2^3))/12$
J	I_{x2}	$(I_{x2})_1 + (I_{x2})_2$
x-axis rotation	Zero	Zero

2.4.3 Modeling of Roof Sheathing

In the original formulation of the stiffness model by Elhouar and Murray (1985), the roof sheathing was modeled as a simple truss with all elements having the same properties. The scope of the research by Elhouar and Murray only included a constant value of the panel shear stiffness. Also, the bending stiffness of the sheathing was neglected and the axial stiffness was not directly evaluated. In the work by Neubert and Murray (1998), the effect of varying panel shear stiffness was investigated. However, the purlin spacing was held constant and the applicable section properties for the truss model were found by trial and error rather than being directly calculated. When the model was extended for use as a design tool, there became a need

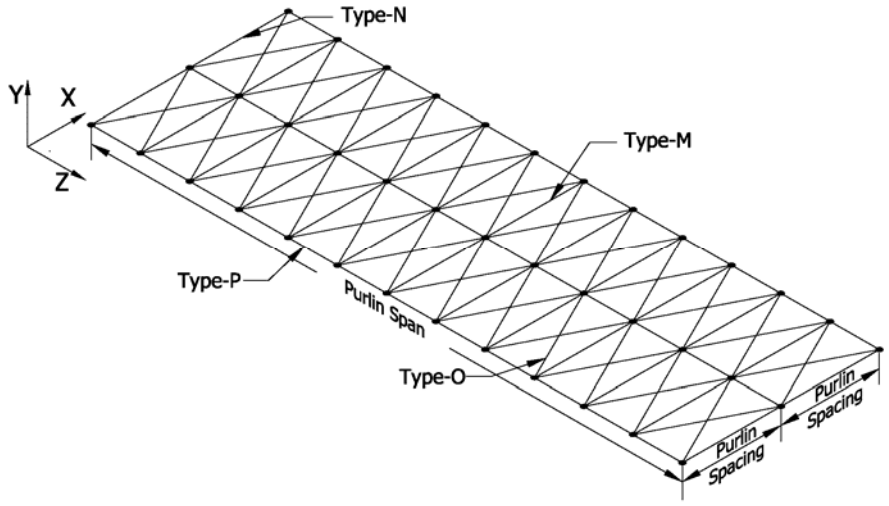

FIGURE 2.3 Panel Truss Elements

to vary the purlin spacing and to directly calculate the properties of the truss members. To accomplish this and to incorporate the bending and axial stiffness of the sheathing, a revised truss model developed by Seek and Murray (2004b) was implemented. This formulation, shown in Figure 2.3, added a second diagonal member to each truss module and used four different section types. The diagonal Type O members were modeled with pinned end truss elements which provide the shear stiffness of the diaphragm. The cross sectional area of the Type O elements was taken as

$$A_O = \frac{G' z(\alpha^2 + 1)^{1.5}}{2E\alpha^2} \tag{2.1}$$

where G' is the shear stiffness of the sheathing, z is the purlin spacing, and α is the module aspect ratio, z/(L/12). The "posts" of the truss were modeled with Type M and Type N elements. The cross sectional area of these elements was calculated to yield the appropriate axial stiffness using the following:

$$A_N = \frac{\sqrt{b^2 + 4ac} - b}{2a} \tag{2.2}$$

$$A_M = 2A_N \tag{2.3}$$

where

$$a = 2zE\alpha(\alpha^2 + 1)^{1.5} \tag{2.4}$$

$$b = 2A_O zE(\alpha^4 + 1) - K_{axial} z^2 \alpha(\alpha^2 + 1)^{1.5} \tag{2.5}$$

$$c = K_{axial} A_O z^2 \tag{2.6}$$

$$K_{axial} = \frac{A_p E}{z} \tag{2.7}$$

and A_p is the cross sectional area of the roof sheathing per unit width. To model the bending stiffness of the sheathing, the Type M and Type N elements were assigned a moment of inertia, I_{zz}, equal to the moment of inertia of the sheathing within the width tributary to the element. Moment releases were added at both ends of the Type M and Type N elements to eliminate bending about the y-y axis and torsion. The longitudinal Type P "chords" of the truss were modeled as axial only truss elements with a cross sectional area of

$$A_p = \alpha A_N \tag{2.8}$$

The above formulation was found to work well for systems with through-fastened sheathing. The test results (Lee and Murray, 2001; Seek and Murray, 2004a) for standing seam systems show a significant reduction in anchorage force when compared to through-fastened systems. This reduction was not seen in the computer model using the above diaphragm model. The transfer of shear forces in a standing seam system is fundamentally different from that of a through fastened system due to slip between the individual panels. To represent this in the model, a hybrid treatment of the panel truss was used. For the effects of the load that acts in the

plane of the purlin web, the sheathing was modeled as described above. Then a separate analysis was executed with the Type O elements removed and the torsional and down slope loads applied. The results of these two analyses were then superimposed.

2.4.4 Modeling of Loads

This research is focused exclusively on the effects of gravity loads. Because gravity loads are applied to the top flange of the purlin via the sheathing and the support reaction acts at the bottom flange, as the purlin deflects laterally, secondary moments will tend to magnify the lateral displacement. For uplift loads, the secondary moments tend to restore the purlin. For these reasons, it is generally accepted that lateral anchorage of purlins under uplift loading is of little concern.

The loads applied to the model are calculated based on an input uniform total roof load distributed with a tributary area approach. In the physical roof system, the gravity loads are applied to the roof sheathing. In the computer stiffness model, the loads are represented by a series of distributed line loads and torsional moments. Typically, the roof system will have some slope; however, the geometry in the computer model is constructed with the plane of the roof parallel to the X-Z plane. To account for the slope, the applied gravity load is separated into vector components acting normal to and in the plane of the roof sheathing, resulting in

$$w_{normal} = w\cos\theta \tag{2.9}$$

$$w_{ds} = w\sin\theta \tag{2.10}$$

The load in the plane of the sheathing, w_{ds}, is applied as a uniform line load acting in the negative X direction along the Type P elements.

The component of the load that acts normal to the sheathing acts in a plane eccentric to the shear center of the purlin and causes torsion in the purlin. The gravity loads are transferred

from the sheathing to the purlin by bearing on the purlin top flange. The true load distribution across the width of the flange is not known. Previous researchers have assumed a triangular distribution, and therefore a resultant force at a distance of b/3 from the purlin web, where b is the width of the purlin flange. During the course of this research it was found that an eccentricity of b/4 agreed better with tests. To model this torsion in the computer stiffness model, a uniform torsion is applied along the length of the Type P elements. The magnitude of this moment is taken as

$$T = w_{normal} \frac{b}{4} \tag{2.11}$$

For sections, such as channels, where the shear center is not located in the plane of the purlin web, the eccentricity is m+b/4, where m is the distance between the shear center and the plane of the web.

For Z-sections the principal axes are inclined with respect to the geometric axes. Therefore, the applied load must be translated into vector components that act in the planes of the principal axes. For this research, this task is handled automatically by the structural analysis software, and is equivalent to taking

$$w_y = w_{normal} \cos\theta_p \tag{2.12}$$

$$w_z = w_{normal} \sin\theta_p \tag{2.13}$$

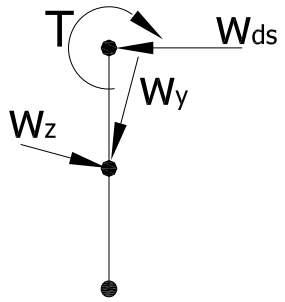

FIGURE 2.4 Summary of Loads

2.4.5 Modeling of the Purlin-to-Sheathing Connection

With the direct consideration of the axial and flexural stiffness of the sheathing included in the model, it was also important to represent the connection between the sheathing and the purlin. Seek and Murray (2004b) proposed using a linear spring in the local y-axis at the top of the Type B and Type F elements with a stiffness of 500 lb/in. to model the flexibility of the clip attachment for the standing seam roofs used in the testing. It was also found through the course of this research, with some communication with Seek and Murray, that including a rotational spring at the ends of the Type M and Type N elements improved the accuracy of the model. It is difficult to quantify the behavior at the sheathing to purlin connection and to establish stiffness values for these springs, as the behavior is complex and very sensitive to the connection details and loading. Simple parametric studies were conducted to assess the sensitivity of the results to changes in the spring constants. The results of a series of models are shown in Figures 2.5 and 2.6. It was found that within a reasonable range the resulting forces were not particularly sensitive to the values of the sliding spring constants. Also, because the primary goal of this research was to develop design tools, and establishing spring constants for all design cases would be impractical, it was preferred that the spring values be held constant. Therefore, the linear spring values were taken as 5,000 lb/in. for standing seam systems and 100,000 lb/in. for through-fastened systems. The parametric studies indicated a greater sensitivity to the values of the rotational spring constant. From the parameter study and by reviewing the correlation of the model results to the test results, a rotational spring constant of 1,500 in.-lb/radian per foot of width was selected for both roofing systems.

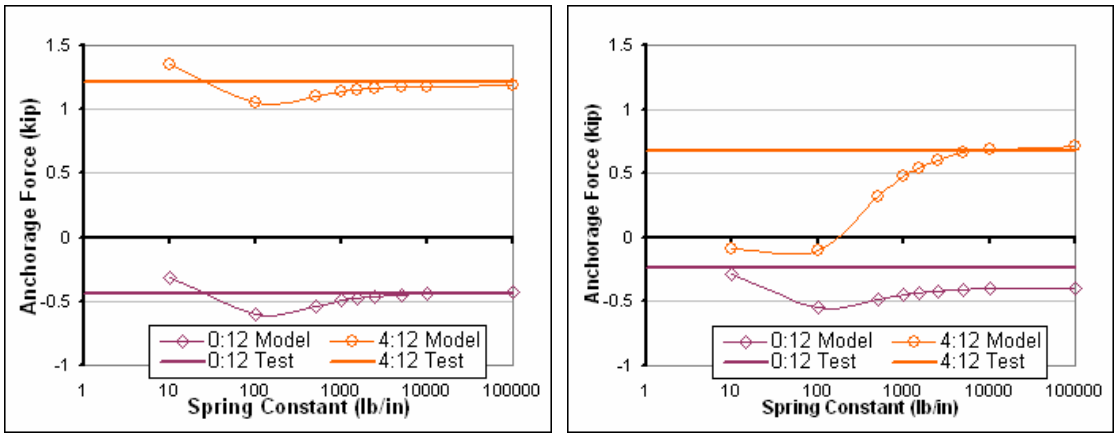

(a) Through Fastened (b) Standing Seam

FIGURE 2.5 Effect of Sliding Spring

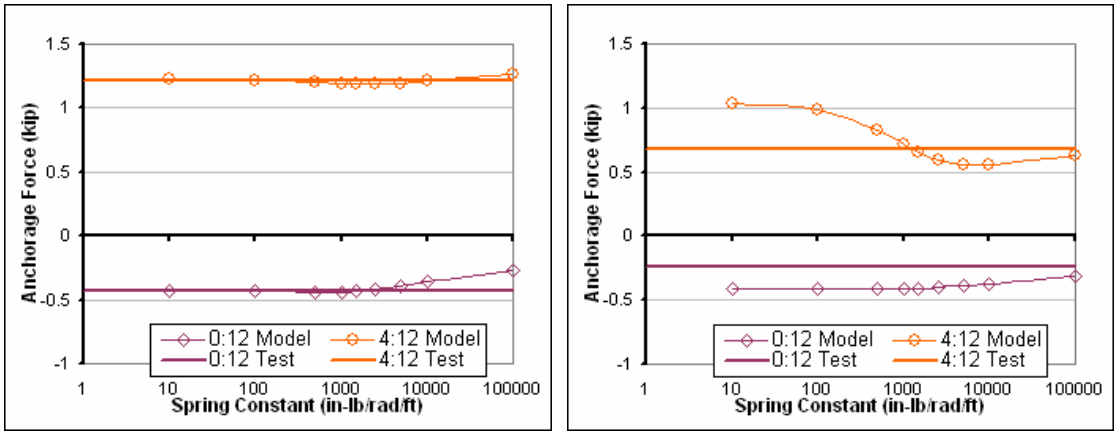

(a) Through Fastened (b) Standing Seam

FIGURE 2.6 Effect of Rotational Spring

2.4.6 Modeling of Anchorage Devices

Murray and Elhouar (1985) and Neubert and Murray (1998) modeled short truss elements spanning from the purlin/sheathing connection to a rigid support to represent the anchors used in the laboratory testing. To extend the applicability of this model to roof systems with multiple anchorage devices throughout the roof system, spring supports were used at the top of the Type B or Type F elements at user selected locations in the model. By using spring supports, the finite stiffness of various anchorage devices can be accurately represented. Due to the indeterminate nature of the roof system, reduction in device stiffness can greatly affect the

predicted anchorage forces. Modeling the points of anchorage with discrete nodal supports accurately represents typical construction details for anchorage devices at the frame lines, and for certain cases when anchorage devices are located along the purlin span. If lines of anchorage are constructed, such as ¼ point anchors connected to a beam at the eave, so that displacement at a line of anchorage is coupled with the displacement of other lines of anchorage, this method of modeling may not correctly represent the constructed system.

2.5 Automation of the Computer Model

With the two goals of the modeling, that is, to develop a design tool and to produce a large matrix of data for calibrating a new manual calculation procedure, it was important for the modeling and analysis to be highly efficient. The management of the modeling data was centered on a Microsoft Excel (2003) workbook with extensive programming using Visual Basic for Applications (VBA). The basic input for each model consists of the building geometry, gravity loads, purlin sizes, sheathing properties, and anchorage device locations and stiffness. When used as a design tool, the user data is input into the Excel worksheet. Alternatively, when large batches of models were needed for the development of the calculation procedure, the data was tabulated in a Microsoft Access (2003) database. A series of subroutines written in VBA within Excel was used to process the basic input and perform calculations to define parameters of the stiffness model. Then an input file for STAADPro (2005) was generated and executed using OpenSTAAD (2005). The resulting forces were then extracted using OpenSTAAD and recorded either in the Excel workbook or in the Access database. For batches of data, this is all executed in a continuous loop where the model was built and executed in as little as five seconds depending on the size of the roof system.

2.6 VALIDATION OF COMPUTER MODEL

To ensure that computer model was accurately replicating the behavior of physical purlin systems, predictions from the computer model were compared to laboratory test results. Testing performed by Lee and Murray (2001) and Seek and Murray (2004a) represented the first work to include the testing of sloped roofs, and provided the primary reference for validating the new computer model.

The test program by Lee and Murray (2001) investigated roof systems with 8 in. and 8.5 in. deep Z-shaped purlins and slopes ranging from horizontal to approximately 17 degrees. Bracing configurations with anchorage points at supports, midpoints, third-points, quarter-points, and third-points plus supports were tested. The roof configurations included simple span systems with two, four, or six purlins and three span systems with four purlin lines. The six purlin tests only included anchorage at the supports. Each configuration was tested with a through-fastened sheathing and a standing-seam sheathing, resulting in eight test series. The computer stiffness model is able to represent all of the test configurations but, for reasons discussed in later sections, this research focused restraints at supports, midpoints, and third points. For each test configuration, a plot of anchorage force versus roof slope was created to graphically represent the correlation between the model and tests. The two examples shown in Figure 2.7 are representative of the results; all cases are presented in Appendix A. Figure 2.8 shows the measured restraint forces from tests versus the restraint force predicted by the stiffness model. The plot shows a fair correlation for both simple span and three-span systems.

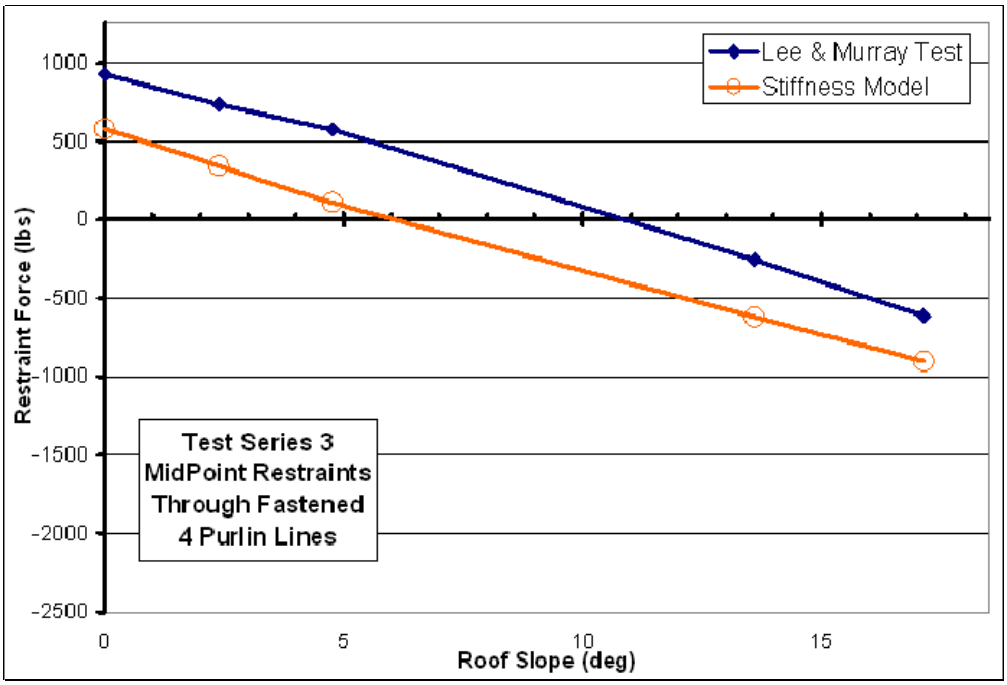

(a) Four Purlin Lines – 8" Z-Purlins– Simple Span
Midpoint Restraints – Through-Fastened Sheathing

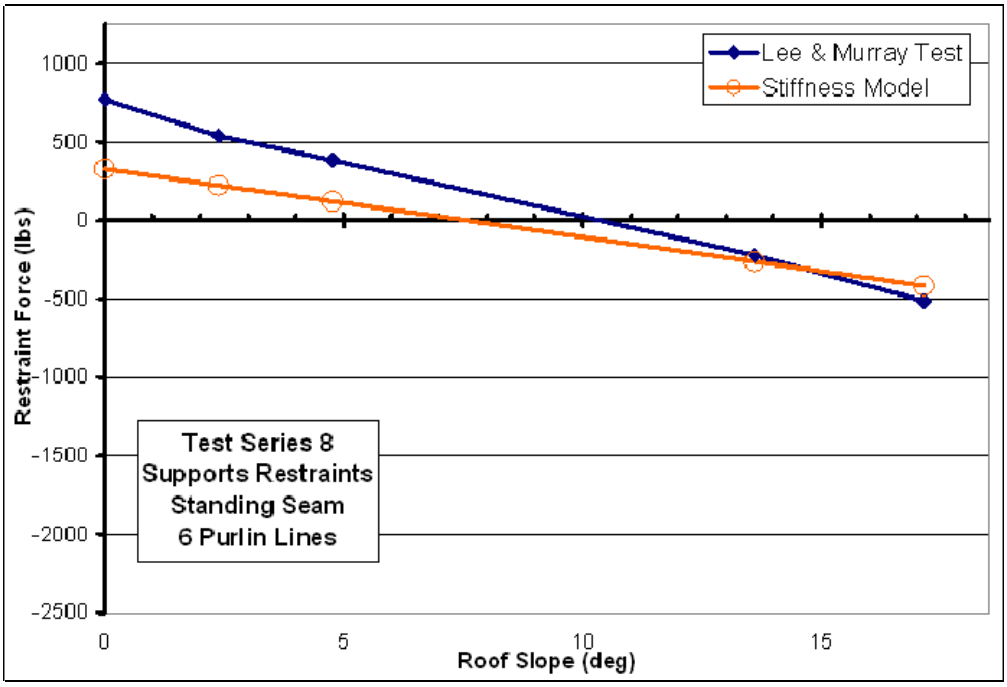

(b) Six Purlin Lines – 8.5" Z-Purlins – Simple Span
Support Restraints – Standing-Seam Sheathing

FIGURE 2.7 Restraint Force vs. Roof Slope
for Computer Model and Lee & Murray Tests

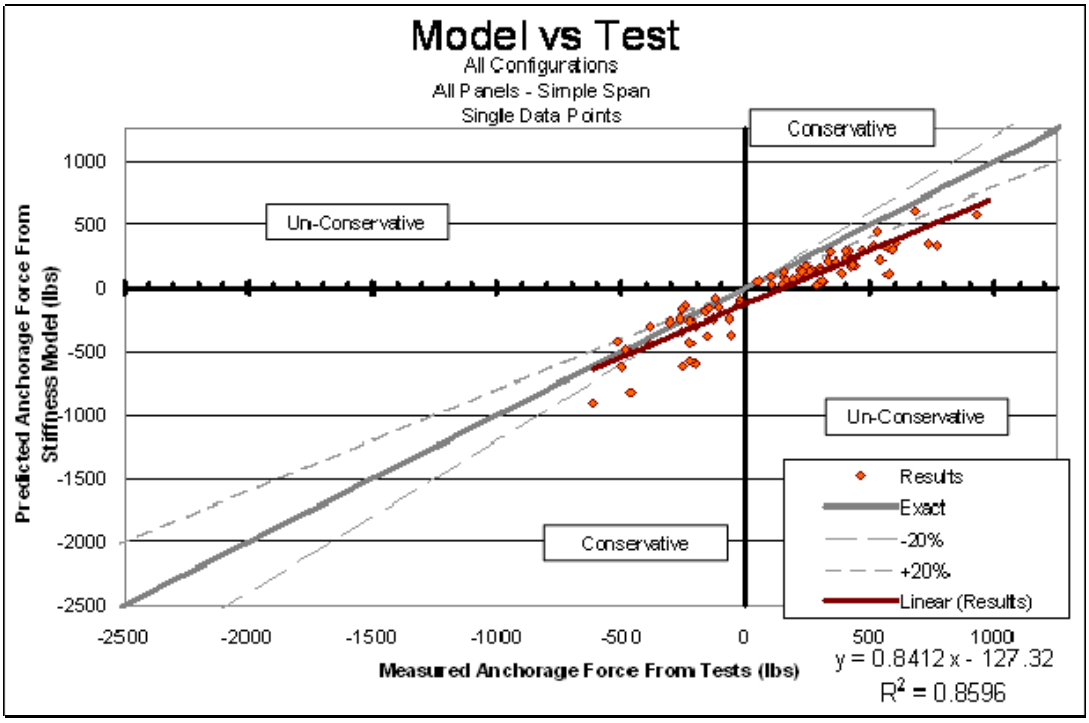

(a) Simple Span Configurations

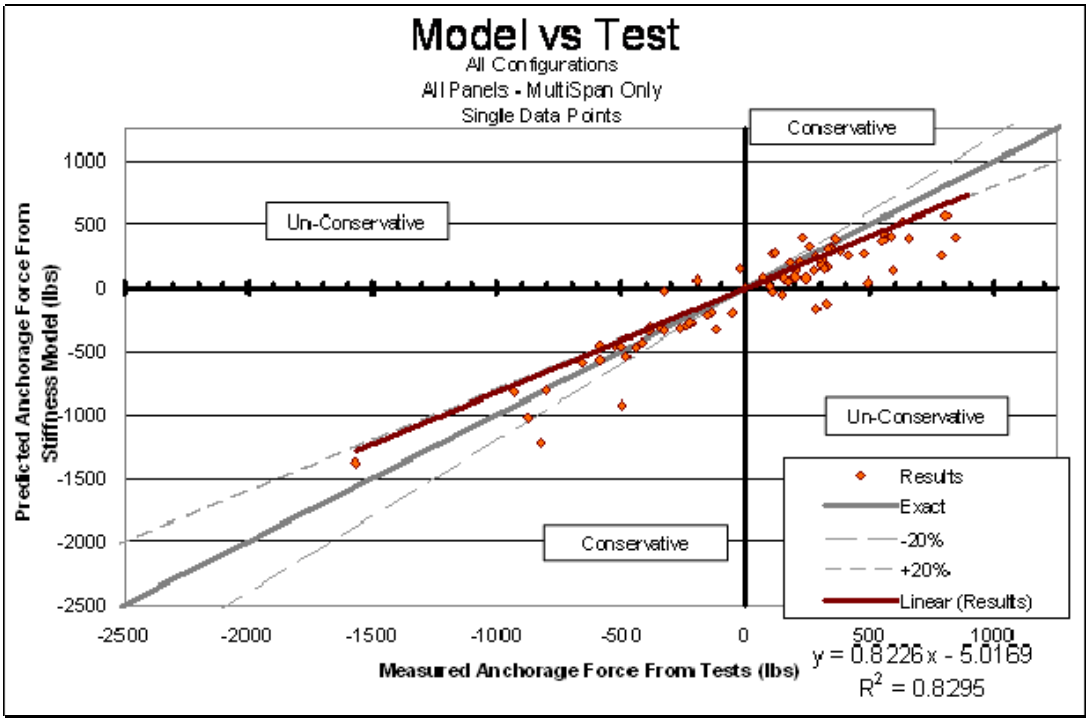

(b) Three-Span Configurations

FIGURE 2.8 Computer Model vs. Lee & Murray Tests

The test program by Seek and Murray (2004a) was similar to that by Lee and Murray but investigated roof systems with 10 in. deep Z-shaped purlins. The roof configurations included simple span systems with two, four, or six purlins and three span systems with six purlin lines. Each configuration was tested with a through-fastened sheathing and a standing-seam sheathing, resulting in eight tests for each bracing configuration. All tested configurations were replicated in the computer stiffness model but, as before, only the supports, midpoint, and third point configurations were considered in depth. The plots of anchorage force versus roof slope are represented in Figure 2.9, with all cases in Appendix B. Figure 2.10 shows the measured restraint forces from tests versus the restraint force predicted by the stiffness model. The plot shows a very good correlation for simple span systems and an acceptable correlation with the three-span systems.

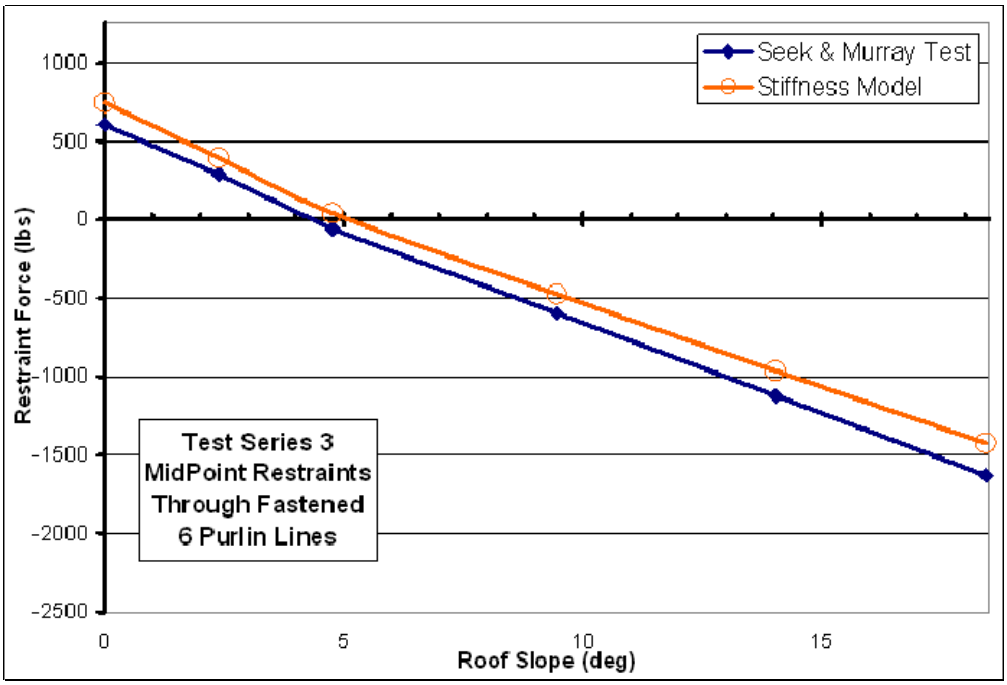

(a) Four Purlin Lines – Simple Span
Third-Point Restraints – Through-Fastened Sheathing

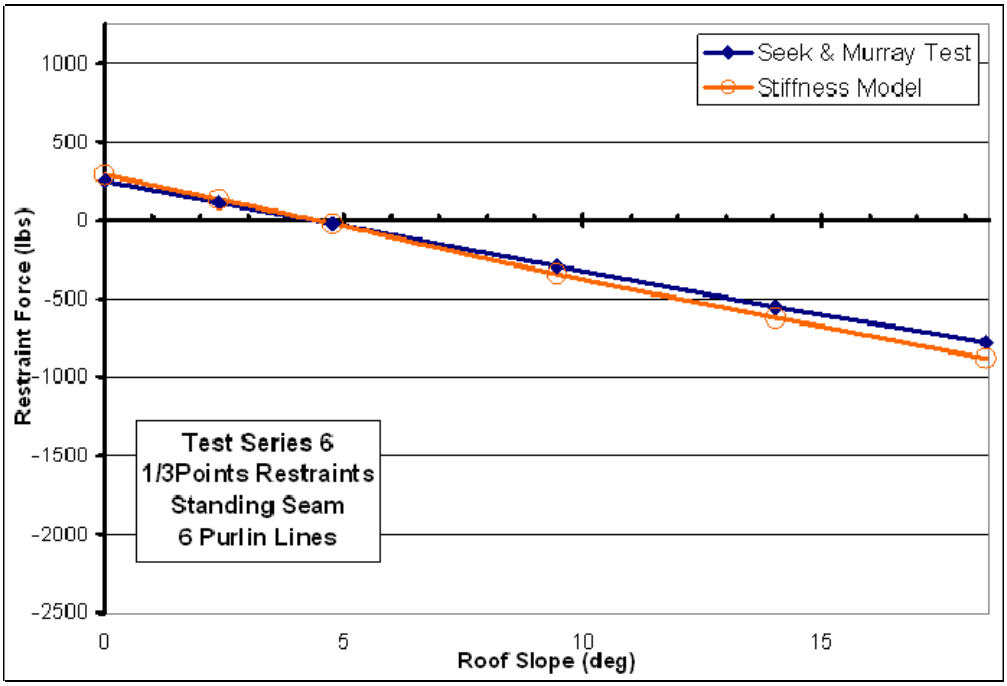

(b) Six Purlin Lines – Simple Span
Third-Point Restraints – Standing-Seam Sheathing

FIGURE 2.9 Restraint Force vs. Roof Slope
for Computer Model and Seek & Murray Tests

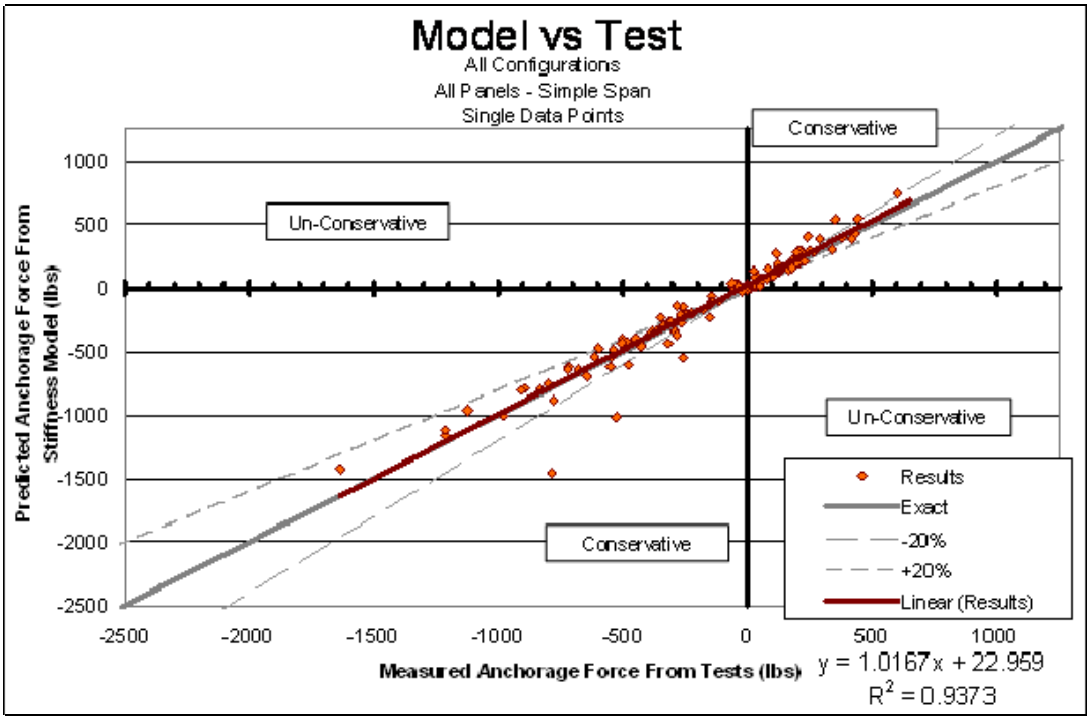

(a) Simple Span Configurations

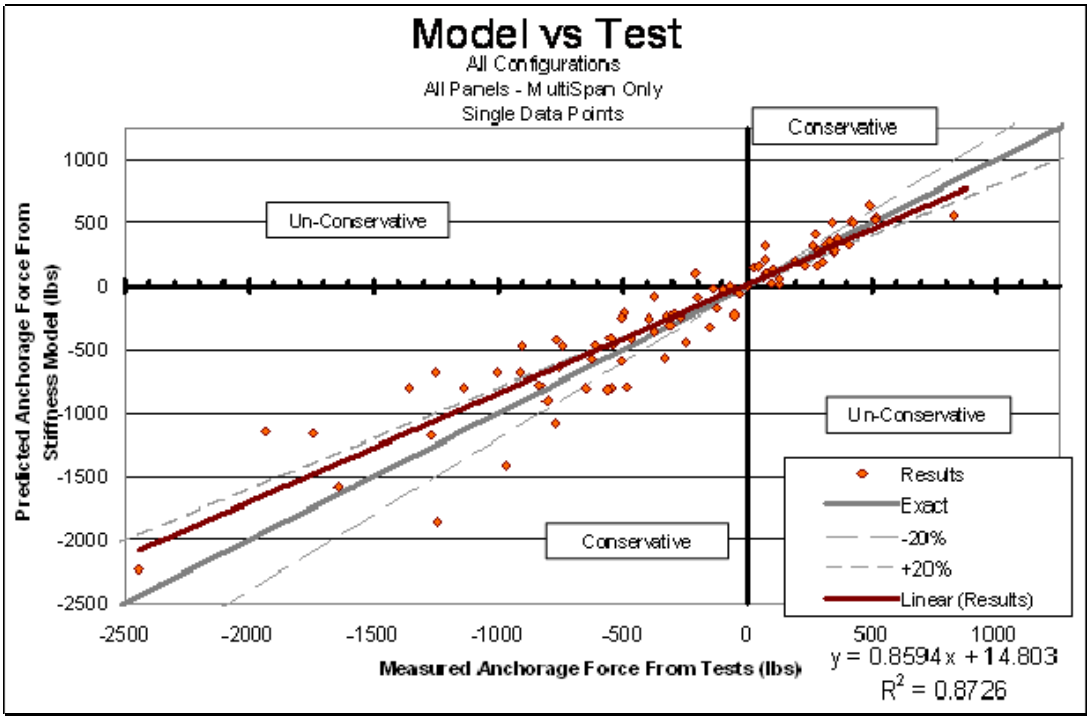

(b) Three-Span Configurations

FIGURE 2.10 Computer Model vs. Seek & Murray Tests

CHAPTER III

FORMULATION OF DESIGN EQUATIONS

3.1 INTRODUCTION

The computer stiffness model presented in Chapter II provides a means to evaluate the lateral anchorage requirements of the majority of metal building roof systems. However, it was also a goal of this research to develop a manual calculation procedure in a form that can be implemented in a design specification. This proposed procedure was developed to address the various deficiencies in the currently available methods, and to better represent the behavior of typical metal building roof systems. The basic formulation of the provisions was based on fundamental mechanics, simplified stiffness analysis, and empirical calibration.

3.2 CURRENT DESIGN PRACTICE

The design of metal building roof systems in North America is guided by the *North American Specification for the Design of Cold-Formed Steel Members* (AISI, 2001). The lateral anchorage force equations given in Section D3.2.1 are based on the work by Elhouar and Murray (1985) with some extension as presented in Equation 1.6. The extension of the original work to sloped roofs resulted in a mistreatment of the system effects. The system effects represent a reduction in the force transferred to an anchorage device due to the inherent resistance to deformation of the purlin system. In the formulation by Elhouar and Murray, the force development due to the eccentricities and inclined axes, and the force reduction due to system effects, were included in the β term. Therefore in the formulation presented in Equation 1.6, no reduction due to system effects is applied to the "sin θ", or down-slope, term.

The work by Neubert and Murray (1998) overcame this shortcoming by separating the force generating effects and the force reducing system effects. However, tests (Lee and Murray, 2001; Seek and Murray. 2004a) have shown that the procedure does not consistently produce an accurate prediction of the anchorage force. Both the Specification equations and the Neubert and Murray equations are based on computer models with a limited number of purlins and anchorage devices located at the low eave. In design practice, multiple anchorage devices may be used and located at various locations throughout the roof. This results in forces being distributed among each of the anchorage devices and changes the behavior of the system effect. No acceptable procedures have been developed to extend either of the methods to address this condition. Also the anchorage devices were modeled as short truss elements connected to rigid supports, which emulated the supports used in laboratory testing. This modeling resulted in very stiff anchorage devices that are not necessarily representative of those used within the industry. As the flexibility of the anchorage devices is varied, the distribution of forces among anchors and the role of the system effect are greatly affected. Because the manual calculation procedures were built around rigid anchorage devices, this behavior is not represented.

3.3 FORMULATION OF EQUATIONS

To overcome the deficiencies noted above, the procedure developed in this research built on the concepts of a single purlin anchorage force, similar to P_o in Equation 1.8, and a relative stiffness technique to distribute the forces. By separating the force terms from the distribution effects, the role of the roof slope is correctly addressed. The relative stiffness technique addresses the stiffness and location of each of the anchorage devices, as well as the interaction of the anchorage devices and the system effect. The technique utilizes a distribution factor that is found by taking the ratio of the effective stiffness of the anchor under consideration to the total

stiffness of all elements providing support to the purlin. This results in the basic design equation

$$P_{L_j} = \sum_{i=1}^{Np} \left(P_i \frac{K_{eff\ i,j}}{K_{total\ i}} \right) \tag{3.1}$$

where P_{Lj} is the anchorage force resisted by the j^{th} anchorage device. The other terms are as presented below.

3.3.1 Single Purlin Restraint Force, P

The above formulation is centered on the concept that the force, P_i, is the anchorage force at the i^{th} purlin if all purlins are directly supported by rigid anchorage devices. This single purlin force is composed of three primary components: a term due to the loading oblique to the principal axes, a term for loading eccentric to the shear center, and a term for the loading component perpendicular to the plane of the web. Neubert and Murray (1998) attempted to derive the value (called P_o in their work) based on the mechanics of a simplified free-body diagram. This simplification neglected the moments developed at the purlin-to-sheathing connection and the purlin-to-rafter connection. To overcome the errors introduced by this simplified model, a semi-empirical approach was used for this research.

To determine the key terms that should be included in the force calculation, a small parameter study was performed, using the computer stiffness model. The work on calibrating the stiffness model had shown that the variation of the anchor force with roof slope is linear, so for the purposes of this study, only 0.25:12 and 4:12 roof slopes were used. The basic model used for this study was the Series 7 system from the testing by Seek and Murray (2004a), except a rigid anchor was provided at every purlin location to eliminate the force distribution effects. Each parameter was varied across a range of five values, while all other parameters were held constant. The results from each set of models were then plotted to provide a qualitative view of

the significance of that parameter. This led to a short list of parameters that were expected to play a role in the force calculation.

With this short list of parameters, regression analysis was used to quantify the role of each of the terms. Each of the three load components (concentric bending, eccentric torsion, and down-slope loading) were treated separately and assumed to have the basic form

$$P_{PA} = C1 \cdot I_x^{C2} \cdot I_{xy}^{C3} \cdot J^{C4} \cdot t^{C5} \cdot b^{C6} \cdot d^{C7} \cdot L^{C8} \cdot S^{C9} (\cos\theta) \tag{3.2}$$

$$P_T = C1 \cdot I_x^{C2} \cdot I_{xy}^{C3} \cdot J^{C4} \cdot t^{C5} \cdot b^{C6} \cdot d^{C7} \cdot L^{C8} \cdot S^{C9} (\cos\theta) \tag{3.3}$$

$$P_{DS} = C1 \cdot I_x^{C2} \cdot I_{xy}^{C3} \cdot J^{C4} \cdot t^{C5} \cdot b^{C6} \cdot d^{C7} \cdot L^{C8} \cdot S^{C9} (-\sin\theta) \tag{3.4}$$

where P_{PA} is the anchorage force due to loading oblique to the principal axes, P_T is the anchorage force due to loading eccentric to the shear center, P_{DS} is the anchorage force due to the roof slope, I_x is the purlin moment of inertia about the geometric major axis, I_{xy} is the product of inertia, J is the torsional constant, t is the purlin thickness, b is the flange width, d is the purlin depth, L is the purlin span, S is the purlin spacing, and C1 to C9 are the independent variables being sought. The regression analysis was run in sets. Following each set, any term that had an exponent near zero was deemed negligible and eliminated. The result of this analysis, with some slight rounding of the exponents to produce equations with consistent units, was the three force component terms

$$P_{PA} = C2 \cdot \frac{I_{xy}}{I_x} \cdot \frac{L}{d} \cdot \cos\theta \tag{3.5}$$

$$P_T = C3 \cdot \frac{b}{d} \cdot \frac{t}{d} \cdot \cos\theta \tag{3.6}$$

$$P_{DS} = -C4 \cdot \sin\theta \tag{3.7}$$

These three terms were then combined in the form

$$P_i = C1 \cdot W_{p_i} \cdot \left[\left(C2 \cdot \frac{I_{xy} L}{I_x d} + C3 \cdot \frac{bt}{d^2} \right) \cos\theta - C4 \cdot \sin\theta \right] \tag{3.8}$$

The formulation up to this point focused on Z-sections. By noting that for C-sections the eccentric loading is simply increased by the distance from the shear center to the mid-plane of the web, the equation can be extended to C-sections. The eccentric loading for Z-sections was taken as b/4, so for C-sections it is m+b/4, where m is the distance from the shear center to the mid-plane of the purlin web. As shown in Figure 1.2, roof systems with C-shaped purlins commonly have some purlins oriented with the open face turned upslope while others are turned downslope. The anchorage force due to the load normal to the sheathing will reverse direction when the purlin orientation is reversed. To account for this effect, the term α, which is either +1 for purlin top flanges facing upslope or -1 for purlin flanges facing downslope, is introduced as shown:

$$P_i = C1 \cdot W_{p_i} \cdot \left[\left(C2 \cdot \frac{I_{xy} L}{I_x d} + C3 \cdot \frac{(m + 0.25b)t}{d^2} \right) \alpha \cos\theta - C4 \cdot \sin\theta \right] \tag{3.9}$$

In low sloped roofs, some Z-purlins along a roof slope may be oriented with the top flange turned downslope to counteract the tendency of the purlins to translate upslope. The implementation of α in Equation 3.9 accounts for resulting forces for any purlin orientation.

3.3.2 Inherent System Stiffness, K_{sys}

Every purlin system has an inherent level of stability and resistance to lateral movement. This resistance comes primarily from the fixity at the purlin-to-rafter connection and the moment resistance at the panel-to-purlin interface. This configuration can be idealized as a column with a fixed base and a rotational spring at the top. By applying the moment of inertia of the purlin web

for out-of-plane bending across an effective width and collecting the constants into the coefficient C5, the lateral stiffness is

$$K = C5 \cdot \frac{ELt^3}{d^3} \tag{3.10}$$

Neubert and Murray utilized a similar formulation for the system effect factor and noted a better correlation with the computer model by using t/d instead of t^3/d^3. During the regression analysis addressed in Chapter IV, a similar effect is demonstrated with the proposed procedure.

3.3.3 Effective Stiffness of Anchors, K_{eff}

The anchorage force generated by each purlin is distributed to each of the supporting elements based on the relative stiffness of each of the elements. When establishing the stiffness of the anchorage devices, it is critical to recognize that the anchors lie in series with the axial behavior of the roof sheathing. Therefore, the stiffness of the anchor, K_a, is effectively reduced because of the axial flexibility of the sheathing. The effective stiffness is then in the form

$$K_{eff_{i,j}} = \left[\frac{1}{K_a} + \frac{d_{p_{i,j}}}{A\,E} \right]^{-1} \tag{3.11}$$

where $d_{pi,j}$ is the distance between the applied load at the i^{th} purlin and the j^{th} anchorage device, and A is the effective cross-sectional area of the roof sheathing. The effective area of the sheathing is dependent on the panel profile and thickness, as well as an effective width. For the proposed calculation procedure, the effective width is taken as some fraction of the purlin span. This fraction is included as part of the C6 coefficient that was determined by regression analysis. With this representation of the area, the effective stiffness is

$$K_{eff_{i,j}} = \left[\frac{1}{K_a} + \frac{d_{p\,i,j}}{C6 \cdot LA_p E} \right]^{-1} \tag{3.12}$$

where A_p is the cross-sectional area of the roof deck per unit width, and L is the purlin span.

For roof systems with multiple purlins and multiple anchor locations, a value of K_{eff} must be calculated for each purlin with respect to each anchor location. The number of K_{eff} terms is then equal to the number of purlins times the number of anchors. The potentially large number of repetitive calculations lends itself to the use of spreadsheets or other computer methods.

3.3.4 Total Effective Stiffness, K_{total}

The denominator of the stiffness ratio in Equation 3.1, K_{total}, represents the total effective stiffness of all elements providing support to a given purlin, including the stiffness of the purlin system and the effective stiffness of every anchorage device, with respect to the purlin. The total effective stiffness is

$$K_{total_i} = \sum_{j=1}^{N_a} \left(K_{eff\,i,j} \right) + K_{sys} \tag{3.13}$$

3.4 MINIMUM STIFFNESS

For an anchorage device to perform properly in a roof system, it must provide a minimum level of stiffness as well as resist the required anchorage force. Because the stiffness of the anchorage device is explicitly considered in the proposed procedure, the condition can be analytically evaluated. However, very little data is available to establish this required level of stiffness. It was decided by the members of the AISI Taskgroup on Anchorage and Bracing that the minimum stiffness should limit the displacement at the anchorage device to approximately 0.5 in. at ultimate loads. This value is based primarily on general observations from tests, rather than direct evaluation.

The formulation presented here does not directly provide the deflection values needed to make the stiffness check for all cases. To develop the stiffness check, two special cases are considered. For a roof system with an anchorage device at only the first purlin, and no system effects, the deflection at the first purlin is

$$\Delta_i = P_{L_i} \Big/ K_a \tag{3.14}$$

with *i* taken as unity. The deflections at subsequent purlins are greater due to the flexibility of the sheathing. This increase mimics the decrease in the value of K_{eff} and indicates that the stiffness reduction included in K_{eff} should be included in the deflection calculation. For a roof system with an anchorage device at every purlin, the deflection at each purlin can be found from Equation 3.14. Multiplying the numerator and denominator in Equation 3.14 by the number of purlins, N_p, produces

$$\Delta_i = N_p P_{L_i} \Big/ N_p K_a \tag{3.15}$$

If system effects are neglected, and the purlins are uniformly spaced, the anchorage force is simply P_i and the numerator is the sum of all P_i terms. If the flexibility of the sheathing is neglected, K_{eff} equals K_a, and the denominator becomes the summation of K_{eff}, or K_{total}. Making these substitutions results in

$$\Delta_i \approx \sum_{i=1}^{N_p} P_i \Big/ K_{total} \tag{3.16}$$

Imposing the deflection limit of d/20, and reorganizing the equation in terms of a minimum stiffness rather than a deflection, results in

$$K_{req} = 20 \cdot \left| \sum_{i=1}^{N_p} P_i \right| \Big/ d \tag{3.17}$$

CHAPTER IV

CALIBRATION OF EQUATIONS

4.1 INTRODUCTION

The design equations presented in Chapter III include six dimensionless coefficients. These coefficients were included to empirically address factors that are difficult to define analytically, such as effective width, and to calibrate the final equations to match the results of the computer stiffness model presented in Chapter II. A series of computer models was developed for each combination of bracing configuration (supports, 1/3-points or mid-points) and each roof sheathing system (through-fastened or standing seam). These models provide the reference data for the non-linear regression analysis that generated the applicable coefficients.

4.2 DEVELOPMENT OF TEST MATRIX

The matrix of computer models used for the regression analysis was developed to represent the wide spectrum of configurations used within the metal building industry and address the variation of each term utilized in the prediction equations. Because the proposed procedure separates the force development from the force distribution, the matrix was also developed to address these two conditions separately.

4.2.1 Roof Configurations for Force Effects

For the calibration of Equation 3.9, which includes the force effects, the values of C1, C2, C3, and C4 are needed. To calibrate these values, in the absence of any force distribution effects, a series of computer models was developed where each purlin was anchored with a rigid anchorage device. In the formulation of the proposed procedure, the values for the purlin spacing, sheathing shear stiffness, and sheathing cross-sectional area were found to be

insignificant. However, to verify that the procedure is applicable to various cases, these variables were included in the matrix. The computer models used in the regression analyis are summarized

Table 4.1 Roof Configurations for Force Effects

Index	Slope (X:12)	Purlin Spaces	Purlin Spacing (ft)	Panel Shear Stiffness (lb/in.)	Sheathing Cross-Sectional Area ($in.^2/ft$)
1	0.125	10	5	*	**
2	0.25	10	5	*	**
3	0.5	10	5	*	**
4	3	10	5	*	**
5	6	10	5	*	**
6	10	10	5	*	**
7	0.125	5	5	*	**
8	0.125	10	5	*	**
9	0.125	20	5	*	**
10	3	5	5	*	**
11	3	10	5	*	**
12	3	20	5	*	**
13	0.125	20	2	*	**
14	0.125	20	3.5	*	**
15	0.125	20	5	*	**
16	0.125	20	6	*	**
17	3	20	2	*	**
18	3	20	3.5	*	**
19	3	20	5	*	**
20	3	20	6	*	**
21	0.125	20	5	60000	**
22	0.125	20	5	25000	**
23	0.125	20	5	10000	**
24	0.125	20	5	2500	**
25	3	20	5	60000	**
26	3	20	5	25000	**
27	3	20	5	10000	**
28	3	20	5	2500	**
29	0.125	20	5	*	0.2744
30	0.125	20	5	*	0.3318
31	0.125	20	5	*	0.367
32	0.125	20	5	*	0.4688
33	3	20	5	*	0.2744
34	3	20	5	*	0.3318
35	3	20	5	*	0.367
36	3	20	5	*	0.4688

* = 25,000 for Through Fastened, 7,500 for Standing-Seam
** = 0.217 for Through Fastened, 0.288 for Standing-Seam

in Table 4.1. For these models, the roof slope, number of purlins, and spacing between purlins are varied while the anchorage and roof sheathing properties are held constant.

4.2.2 Roof Configurations for Distribution Effects

For the force distribution effects, the values of C5 and C6 are needed. To calibrate these values, models with 78 different roof configurations were investigated (see Table 4.2). For these models, the roof slope, number of purlins, spacing between purlins, cross-sectional area of the sheathing, and stiffness of the anchorage devices was varied, as well as the number and location of the anchorage devices. For example, configuration ten has eleven purlins (ten spaces), and an anchorage device at the second, sixth, and eleventh purlin lines.

4.2.3 Purlin Sections and Spans

Within the metal building industry, most manufacturers utilize proprietary cross sections for their cold formed shapes. However, the *Cold-Formed Steel Design Manual* (AISI, 2003) includes standardized sections for reference. For this research, purlin sections were selected from those provided in the AISI Manual. Twenty-two combinations of purlin cross section and span length were selected. For each cross section, two span lengths which are within the range of spans typically used with those sections were chosen. The selected purlins included depths of 6, 8, 10, 12, and 14 in. For the 8, 10, and 12 in. sections, the thickest and thinnest published sections were included. To provide a very slender and a very compact section, the thickest 6-in. and the thinnest 14-in. sections were used. For the 10-in. sections, the flange width was also varied among three values (see Table 4.3). For each combination, a single-span and a five-span model were created. The five-span model allowed for the investigation of an end frame, a first interior frame and a typical interior frame condition for support restraints, and an end bay, first interior bay, and typical interior bay for mid-point and third-point restraints.

Table 4.2 Roof Configurations for Distribution Effects

Index	Slope (X:12)	Purlin Spaces	Purlin Spacing (ft)	Restaint Locations	Panel Shear Stiffness (lb/in.)	Sheathing Cross-sectional Area ($in.^2$/ft)	Restraint Stiffness (kip/in.)
1	0.125	5	5	6	*	**	30kpi
2	0.125	5	5	3	*	**	30kpi
3	0.125	5	5	2,4	*	**	30kpi
4	0.125	5	5	3,4	*	**	30kpi
5	0.125	10	5	11	*	**	30kpi
6	0.125	10	5	6	*	**	30kpi
7	0.125	10	5	5,11	*	**	30kpi
8	0.125	10	5	2,10	*	**	30kpi
9	0.125	10	5	3,7	*	**	30kpi
10	0.125	10	5	2,6,11	*	**	30kpi
11	0.125	10	5	2,5,9	*	**	30kpi
12	0.125	10	5	3,6,8	*	**	30kpi
13	0.125	20	5	2,11	*	**	30kpi
14	0.125	20	5	6,15	*	**	30kpi
15	0.125	20	5	9,14	*	**	30kpi
16	0.125	20	5	2,11,21	*	**	30kpi
17	0.125	20	5	6,11,15	*	**	30kpi
18	0.125	20	5	4,11,18	*	**	30kpi
19	0.125	20	5	2,7,15,21	*	**	30kpi
20	0.125	20	5	5,9,14,17	*	**	30kpi
21	0.125	20	5	3,8,14,19	*	**	30kpi
22	0.125	20	5	2,6,11,16,21	*	**	30kpi
23	0.125	20	5	3,7,11,15,19	*	**	30kpi
.24	0.125	20	5	2,5,9,14,17,21	*	**	30kpi
25	0.125	20	5	3,6,9,13,16,19	*	**	30kpi
26	3	5	5	6	*	**	30kpi
27	3	5	5	3	*	**	30kpi
28	3	5	5	2,4	*	**	30kpi
29	3	5	5	3,4	*	**	30kpi
30	3	10	5	11	*	**	30kpi
31	3	10	5	6	*	**	30kpi
32	3	10	5	5,11	*	**	30kpi
33	3	10	5	2,10	*	**	30kpi
34	3	10	5	3,7	*	**	30kpi
35	3	10	5	2,6,11	*	**	30kpi
36	3	10	5	2,5,9	*	**	30kpi
37	3	10	5	3,6,8	*	**	30kpi

* = 25,000 for Through Fastened, 7,500 for Standing-Seam

** = 0.217 for Through Fastened, 0.288 for Standing-Seam

Table 4.2 Roof Configurations For Distribution Effects (continued)

Index	Slope (X:12)	Purlin Spaces	Purlin Spacing (ft)	Restaint Locations	Panel Shear Stiffness (lb/in.)	Sheathing Cross-sectional Area ($in.^2/ft$)	Restraint Stiffness (kip/in.)
38	3	20	5	2,11	*	**	30kpi
39	3	20	5	6,15	*	**	30kpi
40	3	20	5	9,14	*	**	30kpi
41	3	20	5	2,11,21	*	**	30kpi
42	3	20	5	6,11,15	*	**	30kpi
43	3	20	5	4,11,18	*	**	30kpi
44	3	20	5	2,7,15,21	*	**	30kpi
45	3	20	5	5,9,14,17	*	**	30kpi
46	3	20	5	3,8,14,19	*	**	30kpi
47	3	20	5	2,6,11,16,21	*	**	30kpi
48	3	20	5	3,7,11,15,19	*	**	30kpi
49	3	20	5	2,5,9,14,17,21	*	**	30kpi
50	3	20	5	3,6,9,13,16,19	*	**	30kpi
51	0.125	10	4	2,6,11	*	0.195	30kpi
52	0.125	10	4	2,6,11	*	0.217	30kpi
53	0.125	10	4	2,6,11	*	0.288	30kpi
54	0.125	10	4	2,6,11	*	0.367	30kpi
55	3	10	4	2,6,11	*	0.195	30kpi
56	3	10	4	2,6,11	*	0.217	30kpi
57	3	10	4	2,6,11	*	0.288	30kpi
58	3	10	4	2,6,11	*	0.367	30kpi
59	0.125	10	2	2,6,11	*	**	30kpi
60	0.125	10	3.5	2,6,11	*	**	30kpi
61	0.125	10	5	2,6,11	*	**	30kpi
62	0.125	10	6	2,6,11	*	**	30kpi
63	3	10	2	2,6,11	*	**	30kpi
64	3	10	3.5	2,6,11	*	**	30kpi
65	3	10	5	2,6,11	*	**	30kpi
66	3	10	6	2,6,11	*	**	30kpi
67	0.125	10	5	3,6,8	*	**	150kpi
68	0.125	10	5	3,6,8	*	**	75kpi
69	0.125	10	5	3,6,8	*	**	30kpi
70	0.125	10	5	3,6,8	*	**	15kpi
71	0.125	10	5	3,6,8	*	**	10kpi
72	0.125	10	5	3,6,8	*	**	5kpi
73	3	10	5	3,6,8	*	**	150kpi
74	3	10	5	3,6,8	*	**	75kpi
75	3	10	5	3,6,8	*	**	30kpi
76	3	10	5	3,6,8	*	**	15kpi
77	3	10	5	3,6,8	*	**	10kpi
78	3	10	5	3,6,8	*	**	5kpi

Table 4.3 Purlin Sections and Spans

ID	Purlin	Span (ft)
P1	14zs3.25x080	35
P2	12zs2.75x105	35
P3	12zs2.75x105	30
P4	12zs2.75x070	35
P5	12zs2.75x070	30
P6	10zs3.25x105	30
P7	10zs3.25x105	25
P8	10zs3.25x059	30
P9	10zs3.25x059	25
P10	10zs2.75x105	30
P11	10zs2.75x105	25
P12	10zs2.75x059	30
P13	10zs2.75x059	25
P14	10zs2.25x105	30
P15	10zs2.25x105	25
P16	10zs2.25x059	30
P17	10zs2.25x059	25
P18	8zs2.75x105	25
P19	8zs2.75x105	20
P20	8zs2.75x059	25
P21	8zs2.75x059	20
P22	6zs2.25x105	20

4.3 ANALYISIS OF TEST MATRIX

With the parameters for the test matrix selected, a database was created that contained the input data for each of the models. A total of 30,096 models were analyzed. This is the result of three bracing configurations, two panel types, two span types, 22 purlin and span types, and 114 roof configurations. The resulting anchorage forces for these models were collected from the computer stiffness model and tabulated in the database.

The regression analysis of the resulting data was carried out using the non-linear least squares fitting routines of the OrginPro (2006) software package. The proposed procedure was programmed using the software's proprietary language, and the computer stiffness model results

were pulled from the database. The values of the anchorage forces from the test matrix vary greatly in magnitude. However, because the results are linear with the applied load and the applied load was arbitrarily selected as 40 psf, the comparison between the value predicted by the computer model and that predicted by the calculation procedure was not based on the numerical difference in the results, but on the percentage difference. This was done by applying a weighting factor of $1/P_L$ in the regression analysis, where P_L was the force predicted by the computer model. For some of the models, the predicted restraint force is relatively small. In these cases the percent difference between the two predicted values would be very large for an absolute difference of only a few pounds. To avoid overweighting these data points, any configuration where the absolute value of the restraint force from the computer model was less than fifty pounds was excluded.

It can be seen in Equation 3.9 that, because C1 is applied to all terms, no unique solution for the coefficients exists. The term C1 represents a tributary width factor and always has a value of either 0.5 or 1.0. It was included to create more consistency within the other coefficients. A routine was created within OrginPro that calculates the summation of all the P_i values at a line of anchorage. This routine was then used, along with the results from the so-called force models discussed in Section 4.2.1, to find the coefficients C2, C3, and C4.

Then the remaining data points were analyzed using a routine that carries out the complete calculation procedure to find the coefficients C5 and C6. For this round of the analysis, the values of C1 to C4 were held to the values found in the previous analysis. Also, during this analysis, the exponent applied to the ratio t/d in Equation 3.10 was investigated. It was found that using t^2/d^2 produced the best correlation with the model. The resulting coefficients and analysis statistics are presented in Appendix C and the final coefficients are tabulated in Table 4.4. The

values for C2 and C5 found in the regression analysis had a magnitude on the order of 10^{-3}. So a factor of 1000 was added to Equations 3.9 and 3.10 to simplify the tabulation of the coefficients. The resulting equations are

$$P_i = C1 \cdot W_{p_i} \cdot \left[\left(\frac{C2}{1000} \cdot \frac{I_{xy} L}{I_x d} + C3 \cdot \frac{(m + 0.25b)t}{d^2} \right) \alpha \cdot \cos\theta - C4 \cdot \sin\theta \right] \tag{4.1}$$

$$K_{sys} = \frac{C5}{1000} \cdot N_p \cdot \frac{ELt^2}{d^2} \tag{4.2}$$

Table 4.4 Equation Coefficients

(a) Support Restraints

			C1	C2	C3	C4	C5	C6
Simple Span	Through Fastened (TF)		0.5	8.16	32.6	0.992	0.427	0.167
	Standing Seam (SS)		0.5	8.32	27.8	0.612	0.289	0.051
Multiple Spans	TF	Exterior Frame Line	0.5	14.4	6.88	0.943	0.0728	0.085
		First Interior Frame Line	1.0	4.20	18.3	0.995	2.46	0.433
		All Other Locations	1.0	6.80	22.7	0.988	1.83	0.359
	SS	Exterior Frame Line	0.5	1.27	10.8	0.349	2.42	0.246
		First Interior Frame Line	1.0	1.71	69.2	0.775	1.59	0.135
		All Other Locations	1.0	4.30	55.2	0.705	1.36	0.170

(b) Mid-Point Restraints

			C1	C2	C3	C4	C5	C6
Simple Span	Through Fastened (TF)		1.0	7.60	44.4	0.959	0.753	0.419
	Standing Seam (SS)		1.0	7.55	14.6	0.616	0.352	0.176
Multiple Spans	TF	End Bay	1.0	8.27	46.8	0.953	3.11	0.335
		First Interior Bay	1.0	3.60	53.2	0.922	3.88	0.361
		All Other Locations	1.0	5.44	46.0	0.926	3.14	0.305
	SS	End Bay	1.0	7.95	19.3	0.542	2.00	0.0804
		First Interior Bay	1.0	2.49	40.8	0.465	2.56	0.133
		All Other Locations	1.0	4.13	30.6	0.464	2.71	0.146

(c) One-Third Point Restraints

			C1	C2	C3	C4	C5	C6
Simple Span	Through Fastened (TF)		0.5	7.83	42.4	0.976	0.394	0.401
	Standing Seam (SS)		0.5	7.33	21.4	0.729	0.187	0.178
Multiple Spans	TF	End Bay Exterior Anchor	0.5	15.2	17.4	0.978	0.724	0.043
		End Bay Int. Anchor and 1st Int. Bay Ext. Anchor	0.5	2.43	50.4	0.957	0.819	0.200
		All Other Locations	0.5	6.05	40.8	0.962	0.685	0.117
	SS	End Bay Exterior Anchor	0.5	13.2	13.0	0.718	0.591	0.0349
		End Bay Int. Anchor and 1st Int. Bay Ext. Anchor	0.5	0.841	56.4	0.637	0.202	0.137
		All Other Locations	0.5	3.83	45.2	0.646	0.104	0.0143

4.4 VERIFICATION OF PROCEDURE

To assess the effectiveness of the procedure at emulating the results of the computer model, the coefficient of determination, R^2, was reported for each regression analysis. For nearly all configurations, the value of R^2 is greater than 0.90. This indicates a strong relationship between the prediction equation and the computer model results. The few cases where the quality of the prediction is not as good occur in the end spans of multi-span systems, and provisions were added to the procedure to address these cases. To provide a qualitative and visual perspective on the quality of the procedure, plots were created that present the force predicted by the manual procedure versus the force predicted by the computer model. One example is presented in Figure 4.1; all cases are shown in Appendix C. In these plots, data points that fall along the 45 degree diagonal represent cases where the two prediction methods perfectly agree. Data points that are counter-clockwise from this line are conservatively predicted by the procedure, and points clockwise are unconservative. Anchorage forces were also calculated for each of the systems tested by Lee and Murray (2001) and Seek and Murray (2004a) and are presented on the plots in Appendices A and B.

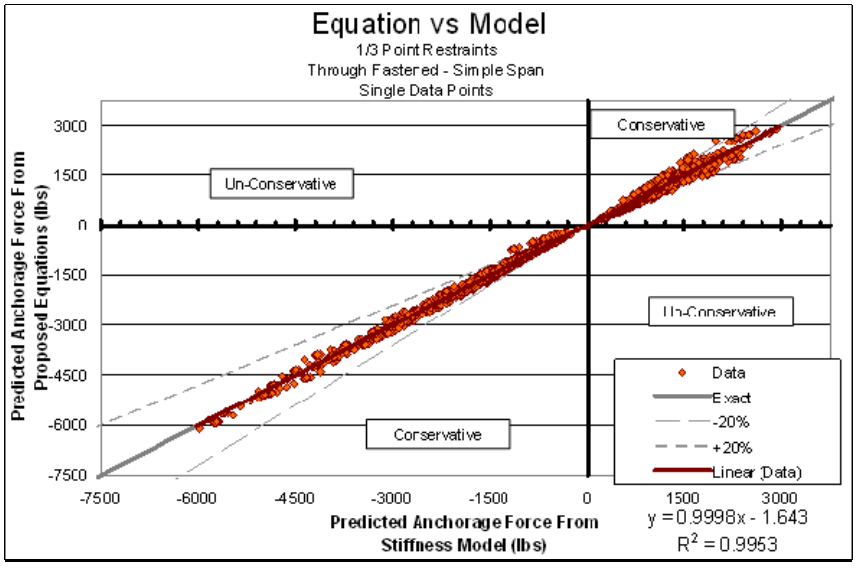

FIGURE 4.1 Calculation Procedure vs. Computer Model

4.5 MATRIX BASED SOLUTION

The design procedure presented up to this point utilizes a relative stiffness technique to distribute anchorage forces. To develop a manual procedure that can be easily presented in a design specification format, the stiffness analysis was simplified slightly and presented in a revised, single-degree-of-freedom format. The same underlying stiffness model can also be solved using matrix methods. This allows for the direct calculation of the displacements and potentially a better evaluation of the minimum stiffness requirements.

To formulate the stiffness model, the forces P_i are applied to nodes representing each purlin. Linear springs connect adjacent nodes and model the axial behavior of the roof sheathing. The stiffness of these springs is related to K_{eff} and can be found from

$$K_{D_k} = \frac{C6 \cdot LA_p E}{S_k} \tag{4.3}$$

where k varies from one to the number of purlin spaces and S_k is the panel span between purlin k and k+1. To simplify the calculations in the manual procedure, the stiffness of all the purlins in the absence of the anchorage devices was collected into a single term K_{sys}. For the matrix solution, K_{sys} is found for each purlin individually and applied as a spring support at the corresponding node. The stiffness of the spring is found by removing the number of purlins, $N_{p,}$ from Equation 4.2, yielding

$$K_{sys}^{*} = \frac{C5}{1000} \cdot \frac{ELt^2}{d^2} \tag{4.4}$$

The resulting model, including a representation of how it was simplified for the manual procedure, is shown in Figure 4.2.

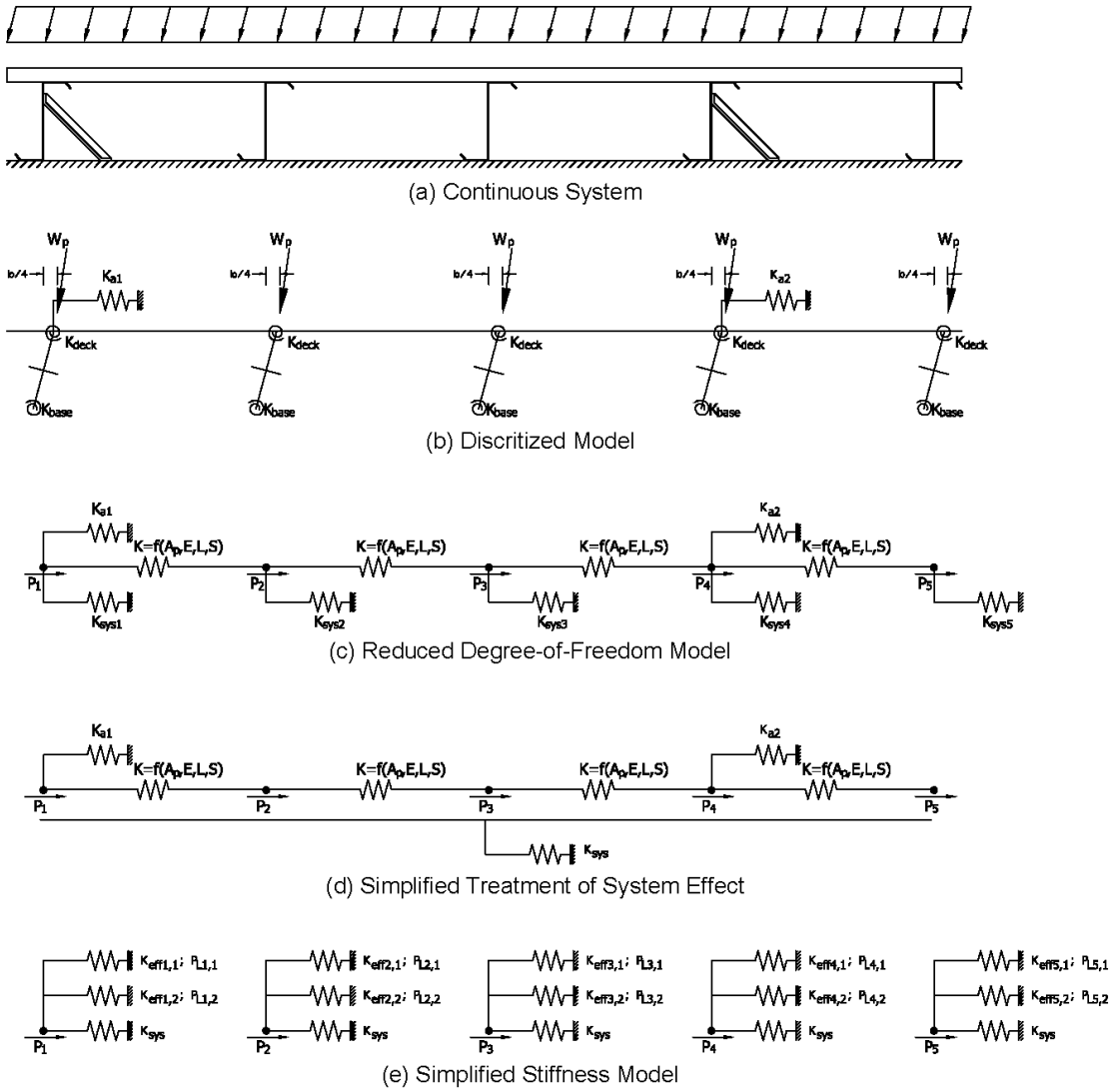

FIGURE 4.2 Summary of Stiffness Model

4.6 APPLICATION TO NON-UNIFORM BAYS

The formulation of the design procedure for multispan systems considered only systems where the purlin size and span length were the same for all bays. In design practice, the bay lengths and purlin sizes will commonly vary along the length of the building. A procedure for extending the design equations to address this condition is considered here.

A series of computer stiffness models was developed to test the behavior of systems with restraints at the supports and mixed bay lengths. The results of these models are summarized in the plots in Figure 4.3 which present the anchorage force (on the vertical axis) at each of the nine frame lines (on the horizontal axis) in the models. The analysis considered a symmetrical configuration having the first two and last two bays with 25 ft spans while the four inner spans have 20 ft spans (see Figure 4.3(a)), as well as an asymmetrical configuration where the first three bays have 25 ft spans while the remaining five bays have 20 ft spans (see Figure 4.3(b)). The first data set in each plot shows the results from the stiffness model with the mixed bays accurately modeled. The second data set shows the anchorage forces from a computer model with all bays modeled as 25 ft, while the third data set has all bays at 20 ft. The intent of these plots is to identify locations where the variation in span length may be neglected, and locations where some averaging technique can be used. It is observed that bays beyond the ones immediately adjacent to the frame line under consideration have relatively little influence on the anchorage force. When a data point from the first model is near a data point for one of the other two computer models, it indicates the procedure should be executed using that span length. The results of the plot qualitatively support the concept of only considering the properties of the two bays immediately adjacent to the frame line.

Since the load, W, the force, P, and the stiffness terms, K_{sys} and $K_{eff,}$ all include the purlin span, L, the problem is non-linear and calculating two anchorage forces and averaging the results produces a different result from averaging the value of the span length prior to using the equations. To select a preferred method, the role of each term was investigated. Equation 4.1 calculates the force generated at each purlin, and because the anchorage force accumulates in the diaphragm in each bay before being transferred to the anchorage device, it is logical to find a

force for the adjacent bays and then average the resulting forces. The system stiffness, $K_{sys,}$ is linear in L, so either averaging the value of the span length, L, or the resulting values of K_{sys} gives the same result. The span length, L, in K_{eff} establishes an effective width for the transfer of the force to the anchorage device. This effective width lies partly in each bay, so using an average span length is more consistent with the intent of the design model. The results of this averaging procedure are shown in the fourth data set in Figure 4.3 and agree well with the results of the complete stiffness model.

When analyzing models with mixed purlin thicknesses, the effects are more complex. Similar plots to those in Figure 4.3 were prepared for systems with different purlin thicknesses along the length of the roof. It can be seen, most clearly in Figure 4.4(a), that the anchorage force is substantially influenced by the purlin properties several bays away. Representing this in the calculation procedure would be extremely complex and require a combined analysis of several (maybe all) of the bays in the roof. The same bay averaging procedure discussed above was considered. The system stiffness, $K_{sys,}$ includes t^2, so unlike above, the result is not the same for averaging the value for the purlin thickness, t, or averaging the resulting values of K_{sys}. Because the source of the system stiffness is the bending of the purlin web due to the moment at the purlin-to-sheathing connection and the moment at the support, it is unclear how it should be handled. It is recommended that average properties be used and Equation 4.4 evaluated once because it yields a slightly conservative result compared to averaging two values of K_{sys}. The results of this procedure are shown in the fourth data set on the plots. While it is not particularly accurate, it is the only practical method available.

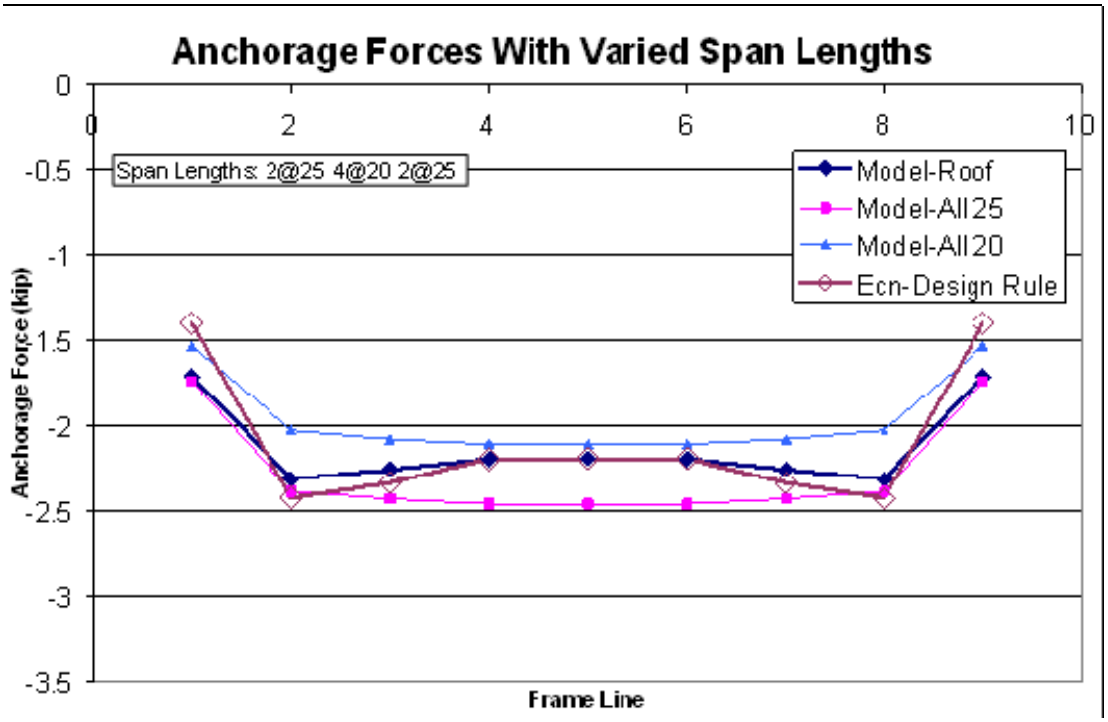

(a) Symmetrical Configuration

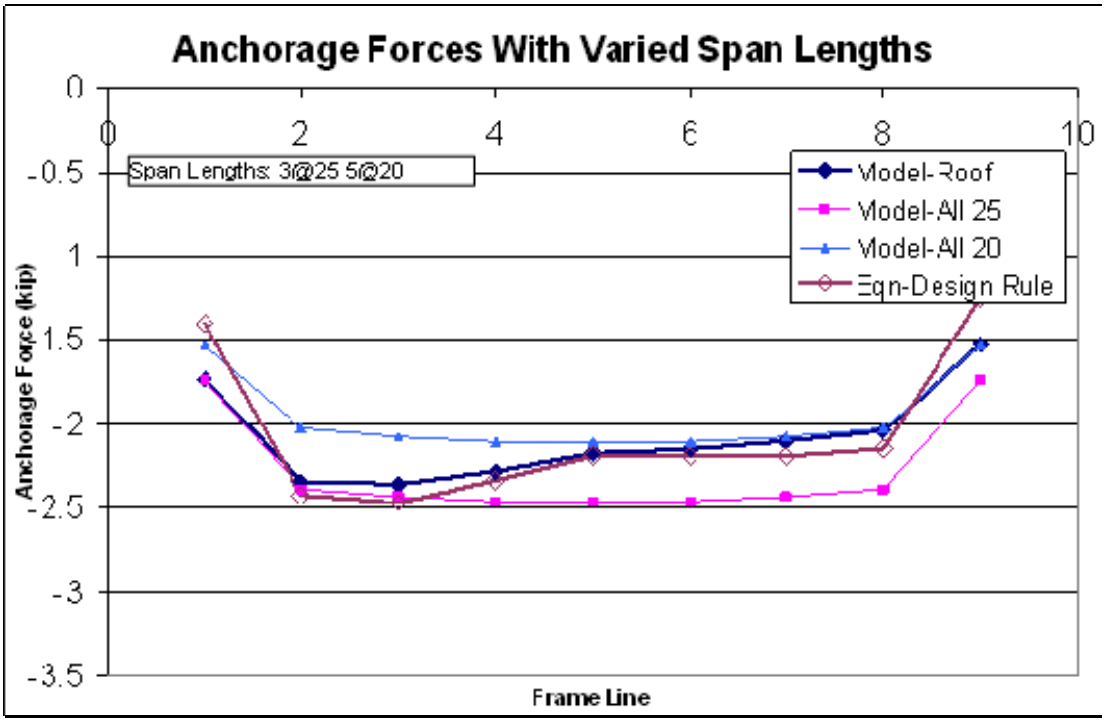

(b) Asymmetrical Configuration

FIGURE 4.3 Anchorage Forces at Support Restraints
in Systems with Varied Span Lengths

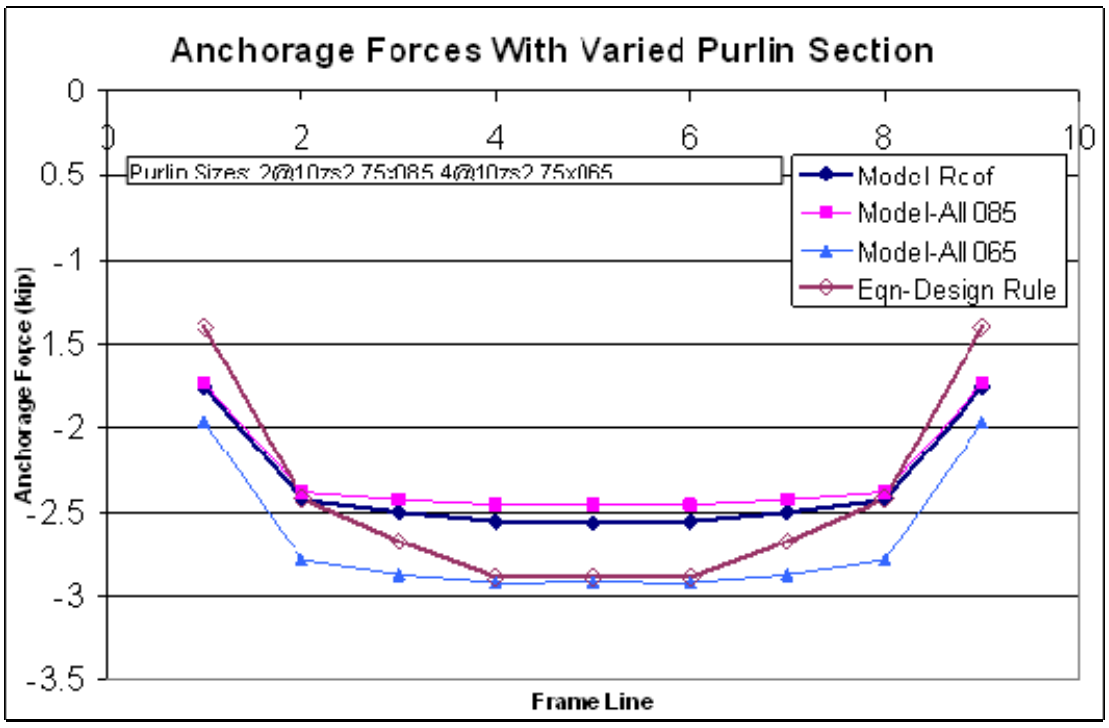

(a) Symmetrical Configuration

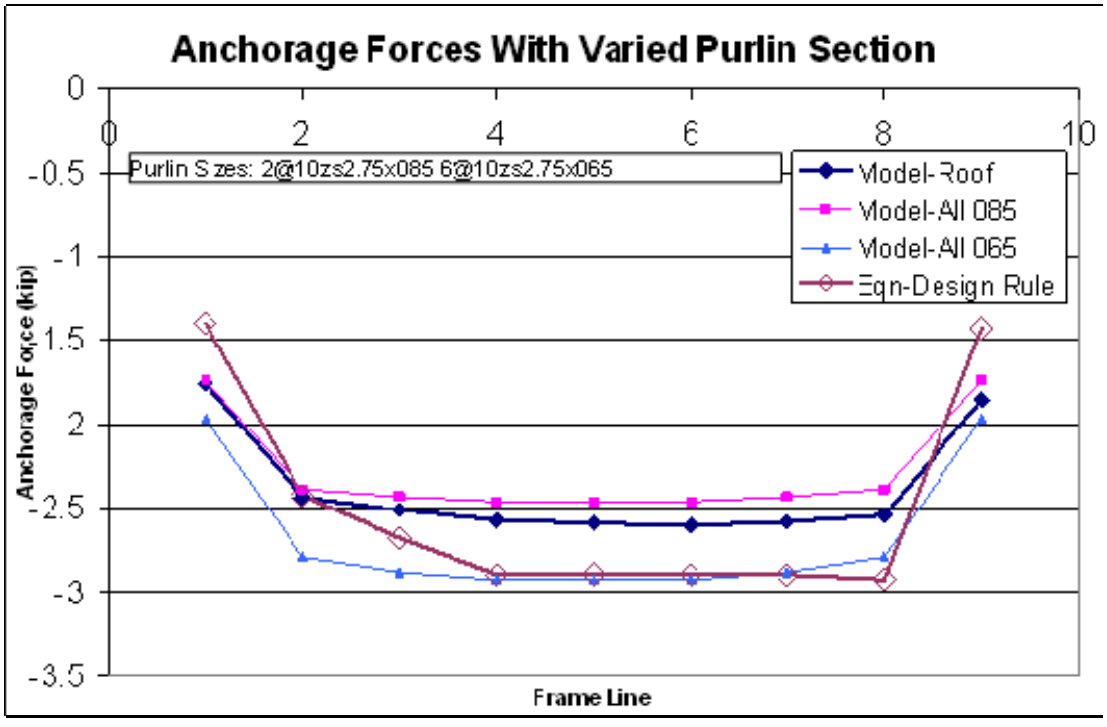

(b) Asymmetrical Configuration

FIGURE 4.4 Anchorage Forces at Support Restraints
in Systems with Varied Purlin Section

A similar evaluation was undertaken for systems with restraints at third points or midpoints. Again the effects of varied span lengths and varied purlin section were considered separately, and two configurations are presented. Figure 4.5 shows how, for points of anchorage where the current bay and the bays to the left and right have the same span length, the anchorage force is essentially the same as that determined from the model with all bays having that span length. For locations where one of the adjacent bays has a different span length, the anchorage force falls between the two values predicted by the uniform bay models. For the cases with varied purlin section shown in Figure 4.6, the results indicate more complex behavior. As with restraints at supports, the change in purlin section affects the anchorage force several bays away. These observations indicate that the calculation procedure should consider the current bay and the bays on either side, and that an averaging technique can be used when the span lengths or purlin properties differ within those three bays.

The same basic procedure discussed for restraints at the supports is applied to restraints at third points or midpoints. The key difference is that now the average needs to be calculated using the three bays involved. Again, the force P_i is to be calculated for each bay and the results averaged. The system stiffness, $K_{sys,}$ is calculated with the average properties of the three bays. Because the effective anchor stiffness, $K_{eff,}$ is concerned with sheathing properties adjacent to the anchor, K_{eff} is calculated with the properties of the current bay. It is recommended that at an end bay, where there is only one adjacent bay, the averages be calculated by adding two times the value from the end bay and the value from the first interior bay, and dividing the sum by three. The results of this procedure are included in the plots in Figures 4.5 and 4.6.

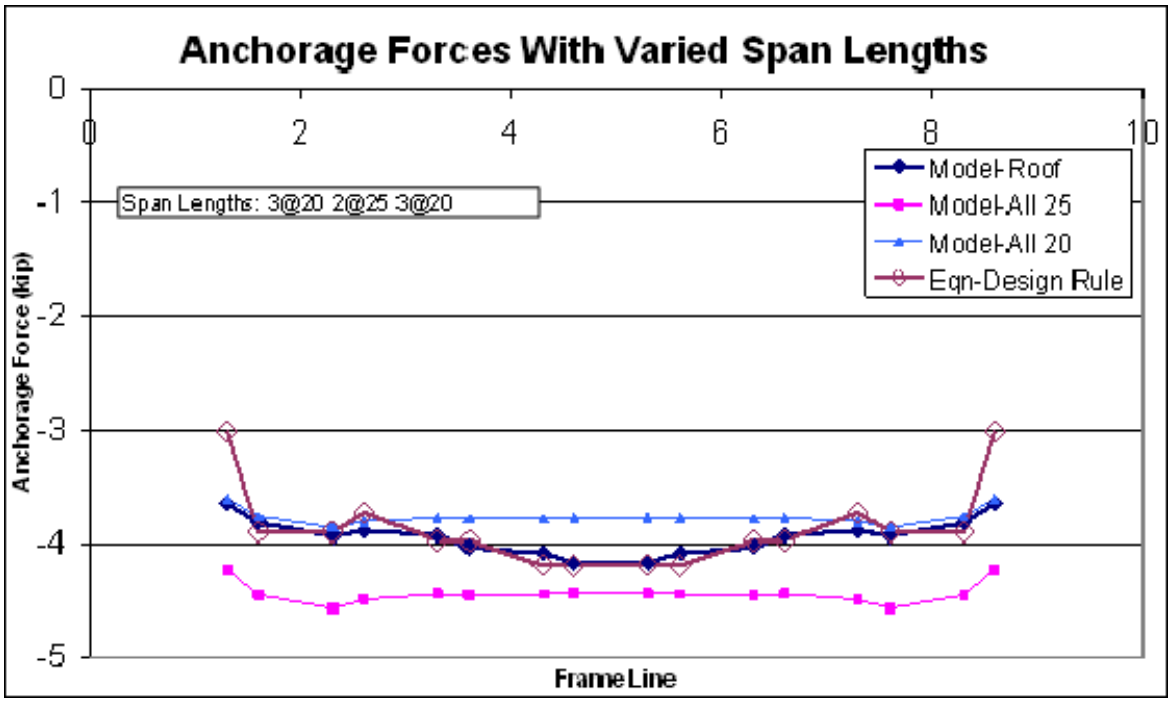

(a) Symmetrical Configuration

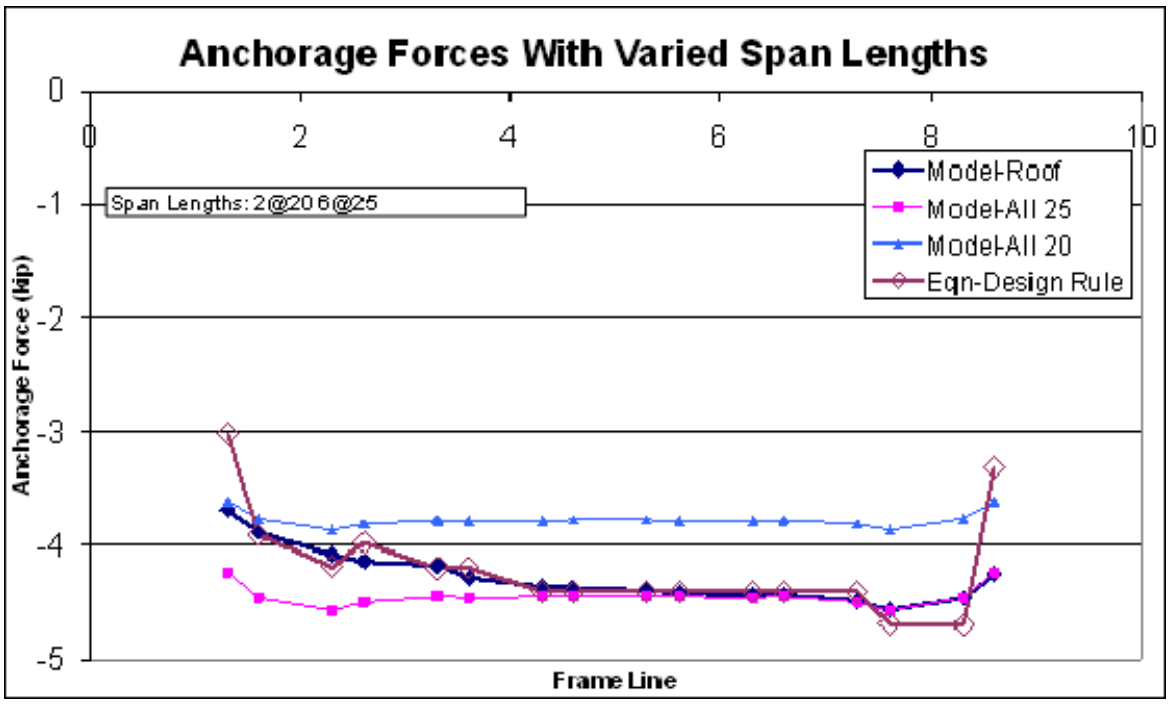

(b) Asymmetrical Configuration

FIGURE 4.5 Anchorage Forces at 1/3 Point Restraints
in Systems with Varied Span Lengths

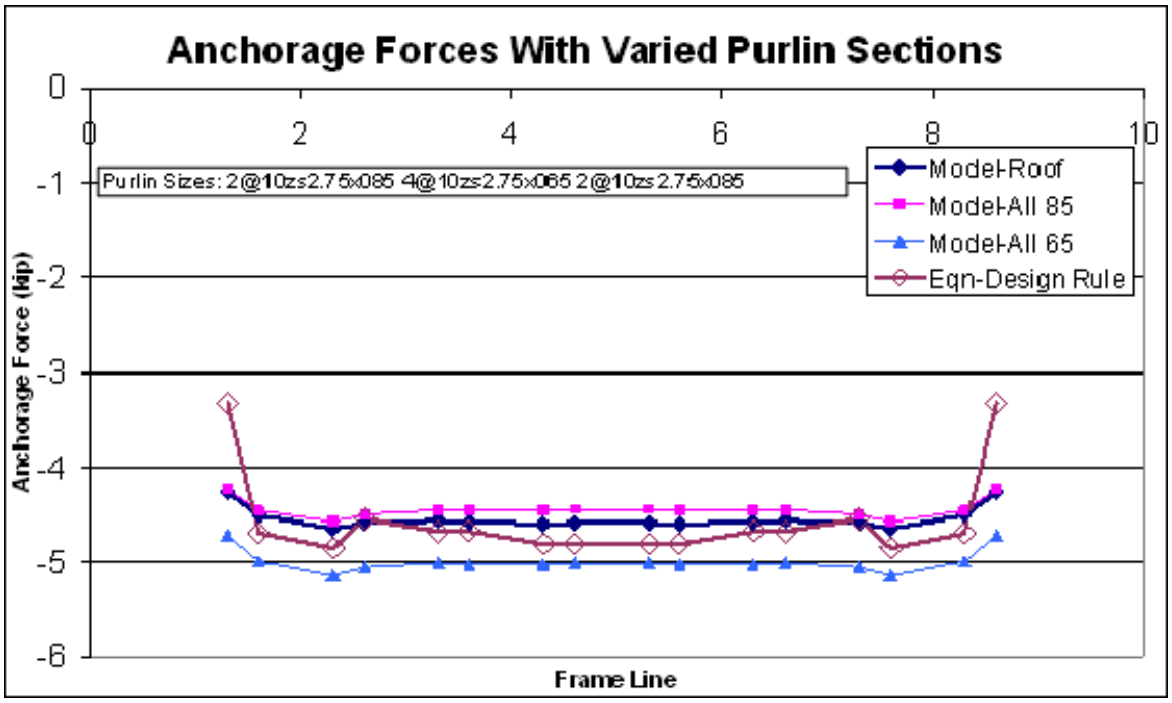

(a) Symmetrical Configuration

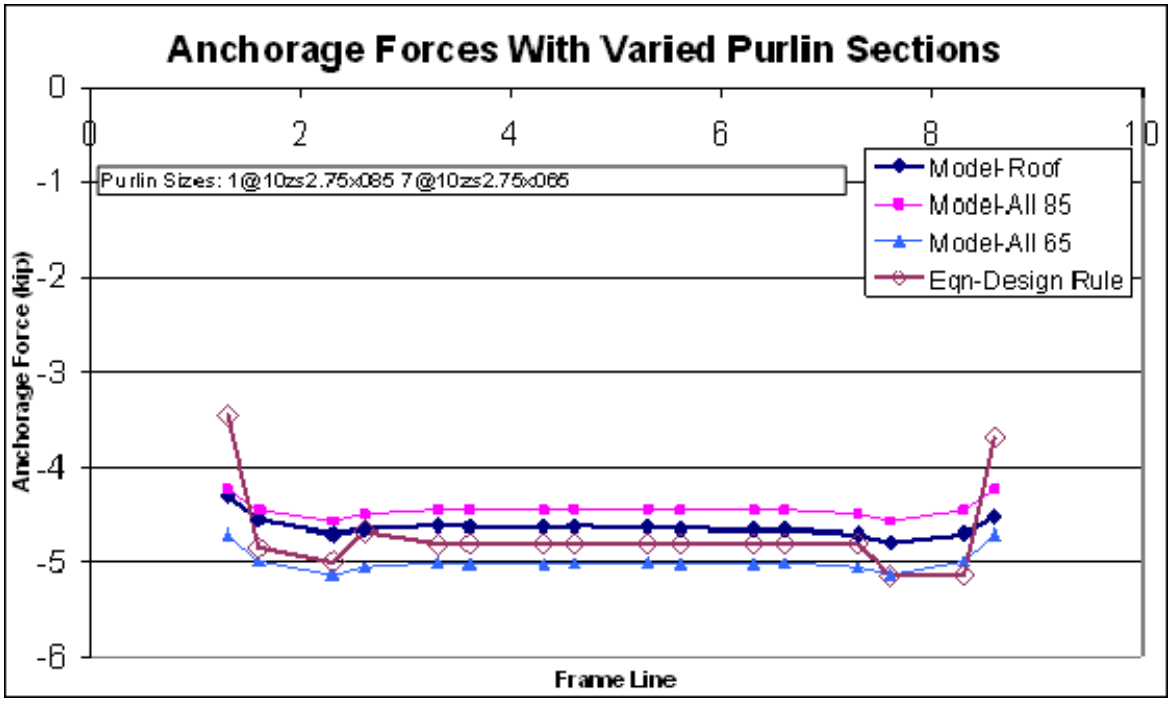

(b) Asymmetrical Configuration

FIGURE 4.6 Anchorage Forces at 1/3 Point Restraints
in Systems with Varied Purlin Section

CHAPTER V

EXAMPLES AND DESIGN RECOMMENDATIONS

5.1 INTRODUCTION

The design equations presented in Chapters III and IV provide a manual calculation method to check the lateral anchorage requirements of metal building roof systems. This chapter provides example calculations to illustrate how the procedure is implemented. Also, various extensions that are required to create a complete design procedure and make it more applicable to conditions encountered in design are presented.

5.2 APPLICATION TO ASD AND LRFD DESIGN METHODOLOGIES

The *North American Specification for the Design of Cold-Formed Steel Members* (AISI, 2001) allows for the design of members at either service level (nominal) loads with Allowable Strength Design (ASD) or at ultimate (factored) loads using the Load and Resistance Factor Design (LRFD) approach. The force calculation in the proposed procedure can be used for either approach by using nominal loads for ASD or factored loads for LRFD. However, for the minimum stiffness requirement, an adjustment is required. The formulation for the minimum stiffness presented in Equation 3.17 is based on limiting the deflection under factored loads. The minimum stiffness is compared to the total stiffness provided as found in Equation 3.13. However, in this formulation no adjustment has been made in either equation for the expected variability in the provided stiffness. To make this adjustment, a resistance factor, ϕ, is added to Equation 3.17, resulting in,

$$K_{req} = \frac{1}{\phi} \frac{20 \cdot \left| \sum_{i=1}^{N_p} P_i \right|}{d} \tag{5.1}$$

To adjust the equation for ASD, a factor of safety, Ω, is used and

$$K_{req} = \Omega \frac{20 \cdot \left| \sum_{i=1}^{N_p} P_i \right|}{d} \tag{5.2}$$

It is recommended that ϕ be taken as 0.75 and Ω as 2.0 unless testing of the anchorage device indicates that different values are more appropriate.

5.3 ILLUSTRATIVE DESIGN EXAMPLES

Example 1: Check the anchorage requirements for a system of four simple span 10ZS3.25x105 purlins spanning 20 ft with a horizontal spacing of 5 ft on center and all top flanges facing up-slope. The roof slope is 3:12 and the factored gravity load is 40psf. The system has restraints at the 1/3 points on the last (high side) purlin line. The anchorage devices have an equivalent horizontal stiffness of 30 kip/in. The roof sheathing is a through fastened deck with a cross sectional area of 0.265 in.^{2}/ft. Use the LRFD approach.

Solution:

From Table 4.4(c) the applicable coefficient values are

C1	C2	C3	C4	C5	C6
0.5	7.83	42.4	0.976	0.394	0.401

The single purlin force is given by Equation 4.1:

$$P_i = C1 \cdot W_{p_i} \cdot \left[\left(\frac{C2}{1000} \cdot \frac{I_{xy} L}{I_x d} + C3 \cdot \frac{(m + 0.25b)t}{d^2} \right) \alpha \cos\theta - C4 \cdot \sin\theta \right] \tag{4.1}$$

For the 10ZS3.25x105 purlins, I_{xy} = 8.41 in.^{4}, I_x = 28.4 in.^{4}, m = 0, d = 10 in., b = 3.25 in., t = 0.105 in., L = 20 ft, α = 1, θ = 14.04°, and the uniform gravity load is distributed to each purlin based on the tributary area as follows:

$$W_{p_1} = W_{p_4} = (2.5\,ft)(40\,psf)(20\,ft)(^{1kip}/_{1000lb}) = 2.0kip$$

$$W_{p_2} = W_{p_3} = (5\,ft)(40\,psf)(20\,ft)(^{1kip}/_{1000lb}) = 4.0kip$$

Thus

$$P_1 = P_4 = 0.5(2)\left[\left(\frac{7.83}{1000}\frac{(8.41)(20\cdot 12)}{(28.4)(10)} + 42.4\cdot\frac{(0+0.25(3.25))(0.105)}{10^2}\right)(1)\cos(14.04) - (0.976)\sin(14.04)\right]$$

$$P_1 = P_4 = -0.148kip$$

and

$$P_2 = P_3 = -0.148\frac{4}{2} = -0.296kip$$

The system stiffness is found from

$$K_{sys} = \frac{C5}{1000}\cdot N_p\frac{ELt^2}{d^2} \tag{4.2}$$

where Np = 4 and E = 29,500 ksi, so

$$K_{sys} = \frac{0.394}{1000}\cdot 4\cdot\frac{(29500)(20\cdot 12)(0.105^2)}{10^2} = 1.23\,^{kip}/_{in}$$

The effective stiffness of the anchorage device, relative to each purlin, is found from

$$K_{eff_{i,j}} = \left[\frac{1}{K_a} + \frac{d_{p\,i,j}}{C6\cdot LA_pE}\right]^{-1} \tag{3.12}$$

where K_a = 30 kip/in, A_p = 0.265 in.^{2}/ft, and d_p varies from 15 ft to zero ft plus an adjustment for the roof slope:

$$K_{eff_{1,1}} = \left[\frac{1}{30} + \frac{(15\cdot 12)\,/_{\cos(14.04)}}{0.401(20\cdot 12)(0.265/12)(29500)}\right]^{-1} = 27.55\,^{kip}/_{in}$$

$$K_{eff_{2,1}} = \left[\frac{1}{30} + \frac{(10\cdot 12)\,/_{\cos(14.04)}}{0.401(20\cdot 12)(0.265/12)(29500)}\right]^{-1} = 28.32\,^{kip}/_{in}$$

$$K_{eff_{3,1}} = \left[\frac{1}{30} + \frac{(5\cdot 12)\,/_{\cos(14.04)}}{0.401(20\cdot 12)(0.265/12)(29500)}\right]^{-1} = 29.14\,^{kip}/_{in}$$

$$K_{eff_{4,1}} = \left[\frac{1}{30} + 0\right]^{-1} = 30\,{}^{kip}/_{in}$$

The total stiffness at each purlin is calculated from the results above and the following equation:

$$K_{total_i} = \sum_{j=1}^{N_a}\left(K_{eff\ i,j}\right) + K_{sys} \tag{3.13}$$

This results in

$$K_{total_1} = 27.55 + 1.23 = 28.78\,{}^{kip}/_{in}$$
$$K_{total_2} = 28.32 + 1.23 = 29.55\,{}^{kip}/_{in}$$
$$K_{total_3} = 29.14 + 1.23 = 30.37\,{}^{kip}/_{in}$$
$$K_{total_4} = 30 + 1.23 = 31.23\,{}^{kip}/_{in}$$

The smallest of these stiffness values is compared to the required minimum stiffness from

$$K_{req} = \frac{1}{\phi}\frac{20 \cdot \left|\sum_{i=1}^{N_p} P_i\right|}{d} \tag{5.1}$$

Thus

$$K_{req} = \frac{1}{0.75} \cdot \frac{20(2 \cdot 0.148 + 2 \cdot 0.296)}{10} = 2.37\,{}^{kip}/_{in} < 28.78\,{}^{kip}/_{in} \quad \text{OK}$$

Finally, the anchorage force is found from the basic design equation

$$P_{L_j} = \sum_{i=1}^{Np}\left(P_i \frac{K_{eff\ i,j}}{K_{total\ i}}\right) \tag{3.1}$$

resulting in

$$P_{L_1} = -0.148\frac{27.55}{28.78} - 0.296\frac{28.32}{29.55} - 0.296\frac{29.14}{30.37} - 0.148\frac{30}{31.23} = -0.851 kip$$

This force PL is the force transferred to the anchorage device. The negative sign indicates that the downslope effect dominates the behavior and the force is resisting the tendency of the purlins to move downslope.

Example 2: Repeat Example 1, except add an additional anchorage device at the first purlin.

Solution:

From Example 1,

$P_1 = P_4 = -0.148 kip$

$P_2 = P_3 = -0.296 kip$

$K_{sys} = 1.23 \, {}^{kip}/_{in}$

$K_{eff_{1,1}} = 27.55 \, {}^{kip}/_{in}$
$K_{eff_{2,1}} = 28.32 \, {}^{kip}/_{in}$
$K_{eff_{3,1}} = 29.14 \, {}^{kip}/_{in}$
$K_{eff_{4,1}} = 30 \, {}^{kip}/_{in}$

The effective stiffness of the added anchorage device, relative to each purlin, is found from

$$K_{eff_{i,j}} = \left[\frac{1}{K_a} + \frac{d_{p\,i,j}}{C6 \cdot LA_p E} \right]^{-1} \tag{3.12}$$

resulting in

$$K_{eff_{1,2}} = \left[\frac{1}{30} + 0 \right]^{-1} = 30 \, {}^{kip}/_{in}$$

$$K_{eff_{2,2}} = \left[\frac{1}{30} + \frac{(5 \cdot 12) \, {}^{1}/_{\cos(14.04)}}{0.401(0.265/12)(29500)(20 \cdot 12)} \right]^{-1} = 29.14 \, {}^{kip}/_{in}$$

$$K_{eff_{3,2}} = \left[\frac{1}{30} + \frac{(10 \cdot 12) \, {}^{1}/_{\cos(14.04)}}{0.401(0.265/12)(29500)(20 \cdot 12)} \right]^{-1} = 28.32 \, {}^{kip}/_{in}$$

$$K_{eff_{4,2}} = \left[\frac{1}{30} + \frac{(15 \cdot 12) \, {}^{1}/_{\cos(14.04)}}{0.401(0.265/12)(29500)(20 \cdot 12)} \right]^{-1} = 27.55 \, {}^{kip}/_{in}$$

The total stiffness at each purlin is calculated from

$$K_{total_i} = \sum_{j=1}^{N_a} \left(K_{eff\ i,j} \right) + K_{sys} \tag{3.13}$$

resulting in

$$K_{total_1} = K_{total_4} = 27.55 + 30 + 1.23 = 58.78\ ^{kip}/_{in}$$
$$K_{total_2} = K_{total_3} = 28.32 + 29.14 + 1.23 = 58.69\ ^{kip}/_{in}$$

The smallest of these stiffness values is compared to the required minimum stiffness:

$$K_{req} = 2.37\ ^{kip}/_{in} < 58.69\ ^{kip}/_{in} \quad \text{OK}$$

Finally, the anchorage force is found from the basic design equation

$$P_{L_j} = \sum_{i=1}^{Np} \left(P_i \frac{K_{eff\ i,j}}{K_{total\ i}} \right) \tag{3.1}$$

resulting in

$$P_{L_1} = -0.148\frac{27.55}{58.78} - 0.296\frac{28.32}{58.69} - 0.296\frac{29.14}{58.69} - 0.148\frac{30}{58.78} = -0.435 kip$$

$$P_{L_2} = -0.148\frac{30}{58.78} - 0.296\frac{29.14}{58.69} - 0.296\frac{28.32}{58.69} - 0.148\frac{27.55}{58.78} = -0.435 kip$$

Due to the symmetry of the system, the anchorage force is the same at both locations. However, because of the system effect and the increased total stiffness, the sum of the two values is greater than the force calculated in Example 1.

5.4 MULTISPAN EXAMPLE

Example 3: Find the anchorage forces and verify the required minimum stiffness at the first interior frame line in the 3-span roof shown below. All purlin top flanges face up-slope.

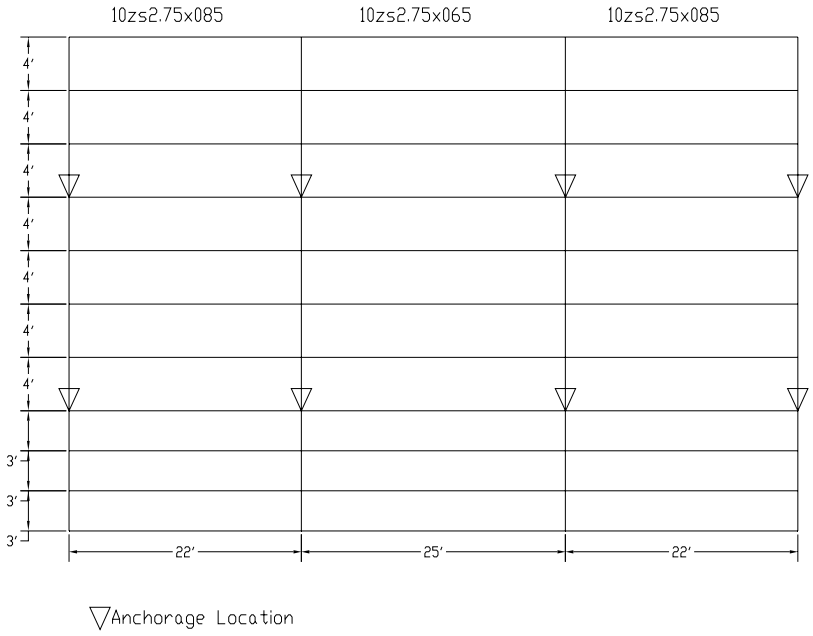

FIGURE 5.1 Example 3 Configuration

The roof slope is 4:12 and the nominal gravity load is 28 psf. The system has restraints at the support points of the 4th and 8th purlin lines, counting upslope from the eave. Each anchorage device has a horizontal stiffness of 40 kip/in. The roof sheathing is a standing seam deck with a cross sectional area of 0.367 $in.^2$/ft. Use ASD.

Solution*:* Due to the repetitive nature of the calculations, several parts of the example are presented in a spreadsheet form. Only the interior frame line is considered here. To check the exterior frame line, the calculations would be repeated with the appropriate coefficients.

From Table 4.4(a) the applicable coefficient values are

	C1	C2	C3	C4	C5	C6
1st Interior Frame Line	1.0	1.71	69.2	0.775	1.59	0.135

The single purlin force is given by Equation 4.1,

$$P_i = C1 \cdot W_{p_i} \cdot \left[\left(\frac{C2}{1000} \cdot \frac{I_{xy} L}{I_x d} + C3 \cdot \frac{(m + 0.25b)t}{d^2} \right) \alpha \cos\theta - C4 \cdot \sin\theta \right] \tag{4.1}$$

where I_{xy} = 5.20 in.^{4}, I_x = 21.0 in.^{4}, t = 0.085 in., and L = 22 ft for the exterior bay, and I_{xy} = 3.96 in.^{4}, I_x = 16.2 in.^{4}, t = 0.065 in., and L = 25 ft for the interior bay. For both bays m = 0, b =2.75 n., d = 10 in., α = 1, and θ = 18.4°. The uniform gravity load is distributed to each purlin based on the tributary area and is shown in Table 6.1. The force considering the exterior bay from equation 4.1 is

$$P_{i\_Ext} = 1.0 W_{p_i} \left[\left(\frac{1.71}{1000} \frac{(5.20)(22 \cdot 12)}{(21.0)(10)} + 69.2 \cdot \frac{(0 + 0.25(2.75))(0.085)}{10^2} \right) (1)\cos(18.4) - (0.775)\sin(18.4) \right]$$

$$P_{i\_Ext} = -0.1956 \cdot W_{p_i}$$

and considering the interior bay

$$P_{i\_Int} = 1.0 W_{p_i} \left[\left(\frac{1.71}{1000} \frac{(3.96)(25 \cdot 12)}{(16.2)(10)} + 69.2 \cdot \frac{(0 + 0.25(2.75))(0.065)}{10^2} \right) (1)\cos(18.4) - (0.775)\sin(18.4) \right]$$

$$P_{i\_Int} = -0.2034 \cdot W_{p_i}$$

The system stiffness is found from

$$K_{sys} = \frac{C5}{1000} \cdot N_p \frac{ELt^2}{d^2} \tag{4.2}$$

where Np = 11, E = 29,500 ksi, L = (22 ft + 25 ft)/2, t = (0.085 in. + 0.065 in.)/2 and d = 10 in:

$$K_{sys} = \frac{1.59}{1000} \cdot 11 \cdot \frac{(29500)(0.5(22 + 25) \cdot 12)(0.5(0.085 + 0.065))^2}{10^2} = 8.18 \, {}^{kip}\!/_{in}$$

The effective stiffness of the anchorage device, relative to each purlin, is found from

$$K_{eff_{i,j}} = \left[\frac{1}{K_a} + \frac{d_{p_{i,j}}}{C6 \cdot LA_p E} \right]^{-1} \tag{3.12}$$

where K_a = 40 kip/in, A_p = 0.367 in.^{2}/ft, and d_p is the distance between the purlin and the anchorage device as shown in Table 6.1.

The total stiffness values shown in Table 6.1 for each purlin are calculated from

$$K_{total_i} = \sum_{j=1}^{N_a} \left(K_{eff\ i,j} \right) + K_{sys} \tag{3.13}$$

Table 6.1 Example 3 Calculations

Purlin Number From Eave (i)	1	2	3	4	5	6	7	8	9	10	11	Ref Eqn
Location (ft)	0	3	6	9	13	17	21	25	29	33	37	
d_p (i,1) (ft)	9.48	6.32	3.16	0.00	4.22	8.43	12.65	16.86	21.08	25.29	29.51	
d_p (i,2) (ft)	26.35	23.19	20.02	16.86	12.65	8.43	4.22	0.00	4.22	8.43	12.65	
Tributary (ft)	1.5	3	3	3.5	4	4	4	4	4	4	2	
Wp_Ext (kip)	0.924	1.848	1.848	2.156	2.464	2.464	2.464	2.464	2.464	2.464	1.232	
Wp_Int (kip)	1.050	2.100	2.100	2.450	2.800	2.800	2.800	2.800	2.800	2.800	1.400	
P_Ext (kip)	-0.181	-0.362	-0.362	-0.422	-0.482	-0.482	-0.482	-0.482	-0.482	-0.482	-0.241	4.1
P_Int (kip)	-0.214	-0.427	-0.427	-0.498	-0.569	-0.569	-0.569	-0.569	-0.569	-0.569	-0.285	4.1
P (kip)	-0.197	-0.394	-0.394	-0.460	-0.526	-0.526	-0.526	-0.526	-0.526	-0.526	-0.263	
Keff (i,1) (kip/in.)	35.32	36.75	38.31	40.00	37.77	35.78	33.99	32.37	30.90	29.55	28.32	3.12
Keff (i,2) (kip/in.)	29.24	30.21	31.25	32.37	33.99	35.78	37.77	40.00	37.77	35.78	33.99	3.12
Sum (kip/in)	64.55	66.96	69.56	72.37	71.77	71.57	71.77	72.37	68.67	65.34	62.31	
Ktotal=Sum+Ksys (kip/in.)	72.74	75.15	77.75	80.56	79.95	79.75	79.95	80.56	76.86	73.52	70.50	3.13
Force to Anchor 1 (kip)	-0.096	-0.193	-0.194	-0.228	-0.248	-0.236	-0.224	-0.211	-0.211	-0.211	-0.106	3.1
Force to Anchor 2 (kip)	-0.079	-0.159	-0.159	-0.185	-0.224	-0.236	-0.248	-0.261	-0.258	-0.256	-0.127	3.1
Force to System (kip)	-0.022	-0.043	-0.042	-0.047	-0.054	-0.054	-0.054	-0.053	-0.056	-0.059	-0.031	

The anchorage forces at each of the two anchorage devices, as well as the force shed to the system effect, are found by taking the sum across all the columns in the last three rows.

PL 1 (kip)	-2.159
PL 2 (kip)	-2.191
PL System (kip)	-0.513
Sum	-4.863

The sum of the three totals is the total force in the system, and is the same value as the sum of the P_i values.

The smallest total stiffness value is compared to the required minimum stiffness from

$$K_{req} = \Omega \frac{20 \cdot \left| \sum_{i=1}^{N_p} P_i \right|}{d} \tag{5.2}$$

Thus,

$$K_{req} = 2 \cdot \frac{20(4.863)}{10} = 19.5 \, {}^{kip}\!/_{in} < 70.5 \, {}^{kip}\!/_{in} \quad \text{OK}$$

CHAPTER VI

SUMMARY AND CONCLUSIONS

6.1 SUMMARY

This research has developed both a three-dimensional stiffness model and a manual analytical procedure to evaluate the lateral anchorage requirements in metal building roof systems. The procedures draw heavily from the work completed by past researchers but overcome several deficiencies in the currently available methods. The computer stiffness model can be used for the analyses of complex anchorage systems and was used to calibrate the manual calculation procedure that predicts the lateral anchorage forces for the majority of situations encountered in the routine design of metal building roof systems. The basic formulation of the calculation procedure builds on the fundamental mechanics of roof purlins and a simplified stiffness analysis to determine the lateral anchorage forces.

The computer stiffness model used here is an extension of the models used by previous researchers with a refined treatment of the roof sheathing and anchorage devices, which resulted in better correlation with tests and a broader applicability to the configurations seen in metal building construction. The manual procedure builds upon the work by Neubert and Murray (1998) with a refined calculation of the basic forces involved and a new stiffness based approach to the distribution and interaction of these forces. Within the formulation of the manual procedure, empirical coefficients are included which calibrate the procedure to the results gathered from the computer stiffness model. Therefore the two procedures are unified and provide similar results where applicable. Additional testing and research may be warranted to address some conditions that are beyond the scope of this project.

6.2 RESTRAINTS AT 1/4 POINTS OR 1/3 POINTS PLUS SUPPORTS

As was mentioned in Chapter II, the development of the calculation procedure dealt with anchorage devices at supports, mid-points, or third-points. There is some interest within the metal building industry for the use of anchorage devices at quarter-points or third-points plus supports. During the development of the computer stiffness model, it was found that the method of providing anchorage devices at quarter-points or third-points plus supports has a substantial influence on the resulting forces. For third-points plus supports, the stiffness of the anchorage devices at the third-points is likely to be very different from the stiffness of the anchorage devices at the supports. For quarter-point restraints, again the stiffness at each line of anchorage differs, but in this condition the behavior of each restraint may be coupled with the behavior of other restraints. If the three lines of anchorage in a quarter point configuration are connected to a beam or truss spanning the bay, displacement at one anchor will cause bending of the beam and impose displacement at the other lines of anchorage. These conditions greatly complicate the analysis and are beyond the scope of this research. If these are modeled properly, the computer stiffness model should provide reasonable results, but this has not been fully investigated. It is recommended that one refer to the work by Seek (2007) if these configurations are to be used.

6.3 WELDED WING PLATES

The laboratory testing that was used to develop the computer stiffness model was conducted with purlins bolted through the bottom flange to the supporting rafter. The purlin to rafter connection may also be made by bolting through the purlin web to a small vertical plate that is welded to the rafter. The procedure developed here does not address this situation. However, with some judgment, it may be applied to systems with these welded wing plates.

If a relatively stiff anchorage point is provided separately from the typical purlin connections, it may be acceptable and conservative to simply ignore the welded wing plates and use the procedure directly. The wing plate connection should provide greater stiffness than the flange bolted connection. Therefore, the system effect would increase and the procedure would yield conservative results. Alternatively, K_{sys} could be modified to include the increased stiffness of the connection. It is difficult to separate the stiffness provided at the purlin-to-sheathing connection from that provided at the rafter support, so it is recommended that any revised K_{sys} be taken as the larger of the value computed in the procedure or the lateral stiffness of the cantilevered plate and purlin at the support.

6.4 TESTING WITH MULTIPLE ANCHORAGE DEVICES

The development of this procedure relied heavily on the laboratory tests by Lee and Murray (2001) and Seek and Murray (2004a) but also extended beyond configurations that were tested. The primary difference between the configurations considered in this research and the laboratory testing is the use of multiple anchorage devices along a line of anchorage. It would be advantageous to conduct laboratory testing to verify the behavior of these configurations. Multi-anchor configurations are highly indeterminate and it may be difficult to determine how the forces are shared between the anchorage devices. If testing is performed, it may be advisable to focus on the measurement of displacements rather than forces. These displacements could then be compared to those generated by the computer stiffness model and the matrix solution form of the calculation procedure.

6.5 CONCLUSIONS AND RECOMMENDATIONS

The design procedure presented here has been developed to address the majority of the conditions encountered in purlin roof systems in the metal building industry. The procedure is applicable to C- and Z-shaped purlins with purlin flanges oriented upslope, downslope, or any combination thereof. Systems with single spans or multiple spans and through-fastened or standing seam roof sheathing may be analyzed. The manual calculation procedure is applicable to configurations with lines of anchorage at the supports, midpoints, or third-points, while the computer stiffness model may be extended with careful modeling to other configuration. The manual procedure represents the first technique for accurately analyzing the behavior of metal building roof systems with sloped roofs or multiple anchorage devices along a line of anchorage. As such, it has been presented to, and approved by, the American Iron and Steel Institute Committee on Specifications for inclusion in the 2007 edition of the *North American Specification for the Design of Cold-Formed Steel Members.* A draft of the specification and commentary is presented in Appendix D.

REFERENCES

American Iron and Steel Institute (2003). Cold-Formed Steel Design Manual, Washington, D. C.

American Iron and Steel Institute (2001). North American Specification for the Design of Cold-Formed Steel Structural Members, Washington D.C.

Elhouar, S. and Murray, T.M. (1985). "Prediction of Lateral Restraint Forces for Z-Purlin Supported Roof Systems," Fears Structural Engineering Laboratory Report No. FSEL/AISI 85-01, University of Oklahoma, Norman, Oklahoma, 107 pages.

MBMA (2006). "Industry Trends: 2006 MBMA Business Review", Metal Building Manufactures Association, Cleveland, OH.

Microsoft Access (2003). Microsoft Corp., Redmond, WA.

Microsoft Excel (2003). Microsoft Corp, Redmond, WA.

Neubert, M. C. and T. M. Murray (1998). "Estimation of Restraint Forces for Z-Purlin Supported, Sloped Roofs Under Gravity Loads," Research Report CE/VPI-ST-99/12, Department of Civil and Environmental Engineering, Virginia Polytechnic Institute and State University, Blacksburg, Virginia, 112 pages.

OpenStaad (2005). Research Engineers Corp., Yorba Linda, CA.

OrginPro (2006). Version 7.5, OrginLab Corp., Northampton, MA.

Seek, M. W. and Murray, T.M. (2004a). "Testing of the Lateral Restraint Force Requirements of Sloped Z-Purlin Supported Standing Seam and Through-Fastened Roof Systems with Two, Four and Six Purlin Lines." Research Report CE/VPI-ST-04/01. Department of Civil and Environmental Engineering, Virginia Polytechnic Institute and State University, Blacksburg, VA, 67 Pages.

Seek, M. W. and Murray, T. M. (2004b). "Computer Modeling of Sloped Z-Purlin Supported Roof Systems to Predict Lateral Restraint Force Requirements." *Conference Proceedings, 17th International Specialty Conference on Cold-Formed Steel Structures.* Department of Civil Engineering, University of Missouri-Rolla. Rolla, Missouri.

Seek, M. W. (2007) "Prediction of Lateral Restraint Forces in Sloped Z-Section Supported Roof Systems Using the Component Stiffness Method" PhD Dissertation, Department of Civil and Environmental Engineering, Virginia Tech, Blacksburg, VA

STAADPro (2005). Research Engineers Corp., Yorba Linda, CA.

Zetlin, L. and Winter, G. (1955). Unsymmetrical Bending of Beams with and without Lateral Bracing, *Proceedings of the American Society of Civil Engineers*, Vol. 81, 774-1 to 774-20.